INFECTION AND IMMUNITY, May 2007, p. 2253–2259 Vol. 75, No. 5
0019-9567/07/$08.00+0 doi:10.1128/IAI.00141-07

Synthesis and Characterization of a Dipalmitoylated Lipopeptide Derived from Paralogous Lipoproteins of *Mycoplasma pneumoniae*▽†

Takeshi Into,[1]‡* Jun-ichi Dohkan,[1]‡ Megumi Inomata,[1] Misako Nakashima,[1] Ken-ichiro Shibata,[2] and Kenji Matsushita[1]

Department of Oral Disease Research, National Institute for Longevity Sciences, National Center for Geriatrics and Gerontology, Obu, Aichi, Japan,[1] and Laboratory of Oral Molecular Microbiology, Department of Oral Pathobiological Science, Hokkaido University Graduate School of Dental Medicine, Sapporo, Japan[2]

Received 28 January 2007/Accepted 12 February 2007

Genomic analysis of *Mycoplasma pneumoniae* revealed the existence of a large number of putative lipoprotein genes compared with the numbers in other bacteria. However, the pathogenic roles of *M. pneumoniae* lipoproteins are still obscure. In this study, we synthesized a lipopeptide (designated *M. pneumoniae* paralogous lipoprotein 1 [MPPL-1]) in which an *S*-dipalmitoylglyceryl cysteine was coupled to a peptide with a consensus sequence of a putative paralogous lipoprotein group characteristic of *M. pneumoniae*. The cytokine-inducing activity of MPPL-1 in human monocytic cells was much weaker (~700-fold weaker) than that of the known mycoplasmal *S*-dipalmitoylated lipopeptide FSL-1 or MALP-2. MPPL-1 required Toll-like receptor (TLR2) to activate NF-κB-dependent gene transcription in HEK293 cells, although a 1,000-fold-larger amount of MPPL-1 was needed to exert activity similar to that of FSL-1 in the cells. TLR2-mediated recognition of MPPL-1 was synergistically upregulated by TLR6 but not by TLR1 or TLR10, although the activity was still weak. In addition, MPPL-1 did not antagonize FSL-1 recognition in human monocytic cells and TLR2/TLR6-expressing HEK293 cells. Thus, these results suggest that there is preferential selective recognition of diacylated lipopeptides due to the magnitude of an affinity with TLR2 and TLR6 and the roles of increased paralogous lipoprotein genes of *M. pneumoniae* in evasion of TLR2 recognition.

Membrane-bound lipoproteins are thought to play important roles in the survival of bacteria through four main functions: a structural function, a transport function, an adhesion function, and an enzymatic function (7). Many lipoproteins have been identified in various species of bacteria and have been shown to comprise a framework structure containing a lipidated N-terminal cysteine residue coupled to distinct polypeptides. The maturation of bacterial lipoproteins generally comprises three steps; the first step involves diacylglyceryl modification of a cysteine residue by diacylglycerol transferase, the second step involves cleavage of the leader peptide by signal peptidase II, and the final step involves N acylation of the N-terminal diacylglyceryl cysteinyl residue, with which lipoproteins are synthesized as triacylated lipoproteins (7). It has also been shown that lipoproteins derived from *Rhodopseudomonas viridis* and several mycoplasmal species do not undergo modification in the final step and are synthesized as diacylated lipoproteins (7).

In contrast to their crucial functions in the survival of bacteria, bacterial lipoproteins act as pathogenic substances to stimulate the immune systems of humans and animals through the recognition receptors that monitor exogenous pathogens (3). Toll-like receptors (TLRs) are central pattern recognition receptors of the innate immune system that recognize a wide range of invading microorganisms through conserved chemical structures in their cells (34). TLR2 is essential for mediation of immune responses to the most diverse set of molecular structures of microbes, including peptidoglycans, lipoteichoic acids, porins, lipoarabinomannans, and lipoproteins/lipopeptides (21, 34). TLR2 forms heteromers with either TLR1 or TLR6, probably to discriminate the structures of molecular patterns, especially the N-terminal lipidated cysteinyl portions of bacterial lipoproteins as active sites (4, 29). TLR1 and TLR6 have been reported to be involved in simple discrimination of the difference between triacylated and diacylated lipoproteins/lipopeptides (36, 37). However, recent arduous work by several study groups has shown that such diverse potentials of TLR1 and TLR6 are largely dependent on more subtle structures of lipoproteins/lipopeptides, such as the length of an N-terminal fatty acid chain, the chirality of the central carbon of the diacylglycerol, and the charge of the C-terminal amino acids (5, 6, 28). It has been suggested that in addition to TLR1 and TLR6, TLR10, which is not encoded in the murine genome, is related to TLR2 recognition because of its sequence similarity and the possibility that it forms a heteromer with TLR2 (8, 12).

Mycoplasmas are microbes in regressive evolution and differ from other microbes in many respects. For example, they completely lack a cell wall, and their bilipid membrane is therefore the only structure that regulates interactions with the external environment (31). Some mycoplasmas cause severe respira-

* Corresponding author. Mailing address: Department of Oral Disease Research, National Institute for Longevity Sciences, National Center for Geriatrics and Gerontology, 36-3 Gengo, Morioka, Obu, Aichi 474-8522, Japan. Phone: 81-562-44-5651, ext. 5064. Fax: 81-562-46-8684. E-mail: into@nils.go.jp.

† Supplemental material for this article may be found at http://iai.asm.org/.

‡ T.I. and J.D. contributed equally to this work.

▽ Published ahead of print on 26 February 2007.

tory, arthritic, and urogenital diseases in humans and animals. *Mycoplasma pneumoniae* is a human pathogen that causes "atypical pneumonia," particularly in older children and young adults (38). The genome size of *M. pneumoniae* is ~820 kb, and the genomic sequence has been completely analyzed (13, 14). Interestingly, a large number of putative lipoprotein-encoding genes have been identified in the genome (46 of 689 genes; 6.68%) compared with the numbers of such genes in the genomes of other microbes, such as *Escherichia coli* K-12 (22 of 4,243 genes; 0.52%) and *Bacillus subtilis* (26 of 4,105 genes; 0.63%) (7). Even in the closely related sister species *Mycoplasma genitalium*, only 21 putative lipoproteins (encoded by 477 genes; 4.4%) could be found. Despite the existence of such genetic data, little is known about the roles of lipoproteins in *M. pneumoniae* pathogenicity, although there has been much interest in the pathogenic roles of membrane lipoproteins of other mycoplasmal species during infection because of their diverse functions, including adherence to host cells, antigenic variation, and TLR2- and TLR6-mediated immunostimulation (30).

In this study, we attempted to synthesize a lipopeptide having an *S*-(2,3-bispalmitoyloxypropyl)-cysteine residue coupled to an N-terminal consensus peptide of *M. pneumoniae*-specific lipoproteins encoded by paralogous genes. Interestingly, the level of immunostimulatory activity of this lipopeptide was much lower than that of the known mycoplasmal lipopeptide MALP-2 or FSL-1 despite the structural uniformity. We also investigated the recognition of this lipopeptide by TLRs.

MATERIALS AND METHODS

Preparation of synthetic lipopeptides. The synthetic lipopeptides FSL-1 and MALP-2 were prepared as described previously (17). *S*-(2,3-bisacyloxypropyl)-cysteinyl TGIQADLRNLIK, designated *M. pneumoniae* paralogous lipoprotein 1 (MPPL-1), was synthesized using a method similar to the method used for synthesis of FSL-1 and MALP-2. Briefly, the side chain-protected sequence TGIQADLRNLIK was constructed with an automated peptide synthesizer (model 433; Applied Biosystems). (9-Fluorenylmethoxy carbonyl)-*S*-(2,3-bispalmitoyloxypropyl)-cysteine (Novabiochem) was manually coupled to the peptide resin by using a 1-hydroxy-7-azabenzotriazole-1-ethyl-3-(3-dimethylaminopropyl)-carbodiimide/CH_2Cl_2-dimethylformamide solvent system. The 9-fluorenylmethoxy carbonyl and resin were removed from the lipopeptide by using trifluoroacetic acid. The lipopeptide was extracted into 90% acetic acid, lyophilized, and purified by preparative high-pressure liquid chromatography with a reversed-phase C_{18} column (30 by 250 mm). The level of purity of the lipopeptide was confirmed by analytical high-pressure liquid chromatography with a reversed-phase C_{18} column (4.6 by 150 mm) to be 96%. All of the lipopeptides were used without separation of the *S*-form and *R*-form stereoisomers. The lipopeptides were dissolved in phosphate-buffered saline containing 10 mM *n*-octyl-β-glucopyranoside at a concentration 0.5 mM and stored at −80°C until they were used.

Cell culture. Dulbecco modified Eagle medium, RPMI 1640 medium, penicillin G, streptomycin, and trypsin-EDTA were obtained from Sigma. Human monocytic cell line THP-1 was cultured in RPMI 1640 medium as described previously (19). Human embryonic kidney HEK293 cells were grown in Dulbecco modified Eagle medium as described previously (18).

Determination of IL-6 and IL-8 by enzyme-linked immunosorbent assays (ELISA). A total of 1×10^5 THP-1 cells were stimulated for 12 h with various concentrations of mycoplasmal lipopeptides, and the amounts of interleukin-6 (IL-6) and IL-8 released into the media were determined by using human IL-6 Cytoset and human IL-8 Cytoset (Invitrogen), respectively, according to the instructions of the manufacturer. The results described below are representative of three separate experiments, and the data are expressed as means and standard deviations.

DNA cloning. Plasmids encoding human TLR1, TLR2, and TLR6 have been described previously (18). Human TLR10 cDNA was obtained by reverse transcription-PCR of RNA isolated from human umbilical vein endothelial cells and then cloned into a pEF6 vector (Invitrogen). The DNA sequences were confirmed by the dideoxy chain termination method by using an ABI Prism 3100 genetic analyzer.

Luciferase reporter gene assay. HEK293 cells were plated at a concentration of 0.5×10^5 cells per well in 24-well plates before transfection. The cells were transiently transfected with an NF-κB-driven firefly luciferase reporter plasmid (pNF-κB-Luc; Stratagene) and a construct directing expression of *Renilla* luciferase under the control of a constitutively active thymidine kinase promoter (pRL-TK; Promega) together with TLR-encoding plasmids. After 24 h of incubation, the cells were stimulated for 6 h with MPPL-1 or FSL-1 in media containing 1% fetal bovine serum. Then the cells were lysed, and the luciferase activity was measured using the Dual-Luciferase reporter assay system (Promega) according to instructions of the manufacturer. The results below, expressed as the means and standard deviations of values for triplicate wells, are representative of three separate experiments. The experiment using HEK293 cells stably expressing TLR2 has been described previously (20).

Statistics. All values were evaluated by statistical analysis using Student-Newman-Keul's test. Differences were considered to be statistically significant at a P value of <0.05.

RESULTS

Preparation of MPPL-1. Himmelreich et al. reported that 46 protein genes were identified as genes encoding putative lipoproteins in the *M. pneumoniae* M129 (=ATCC 29342) genome based on the following characteristic lipoprotein-specific features: (i) the presence of one or more basic amino acids among the first five to seven amino acids of the N terminus, (ii) the presence of a hydrophobic signal peptide, and (iii) the presence of a cysteine residue immediately downstream of the signal peptide (13). However, we found that 48 proteins had these lipoprotein signatures. The N-terminal lipoprotein moieties of all putative lipoproteins are shown in Table S1 in the supplemental material. The amino acid sequences of these lipoproteins are included in the data at a website (http://www.ncbi.nlm.nih.gov/entrez/query.fcgi?CMD=search&DB=genome), and the protein designations were based on the MPN numbering scheme described by Himmelreich et al. (13). Importantly, many of these putative lipoproteins have recently been confirmed to be functionally expressed in the microorganism (11, 33, 39). In addition to 48 putative lipoproteins, there are several proteins with high levels of similarity to the lipoproteins without the lipoprotein signature at the N terminus (13), but we did not include these proteins in the list.

Comparison of 30 amino acids of N-terminal lipoprotein moieties revealed that the *M. pneumoniae* lipoproteins include members of seven subgroups, which are probably groups of paralogous lipoproteins (see Table S1 in the supplemental material). We focused on group 1 composed of MPN011, MPN054, MPN271, MPN369, MPN411, MPN467, MPN650, and MPN654 because the N-terminal sequences of these putative lipoproteins could not be identified by a BLAST search in other known organisms, even the sister species *M. genitalium*, suggesting that the lipoprotein genes were propagated uniquely in the evolution of this microorganism. The sequence of MPN505 is also very similar to the sequences of these lipoproteins, but MPN505 lacks the lipoprotein signature. Importantly, the study of Hallamaa et al. showed that there was expression of mRNAs for all group 1 lipoproteins and the detectable proteins MPN271, MPN411, and MPN650 (11). Comparison of N-terminal sequences of these lipoproteins revealed that the levels of similarity of MPN271, MPN369,

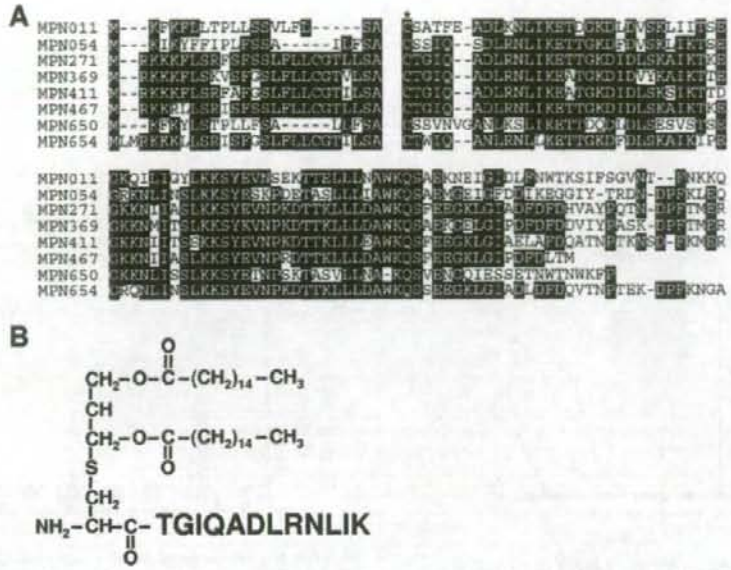

FIG. 1. Synthesis of MPPL-1. (A) Alignment of putative paralogous lipoproteins. The N-terminal sequences of MPN011, MPN054, MPN271, MPN369, MPN411, MPN467, MPN650, and MPN654 were compared. The cysteine residue immediately downstream of the signal peptide is indicated by an asterisk. (B) Structure of MPPL-1.

MPN411, MPN467, and MPN654 are particularly high (Fig. 1A). These putative lipoproteins have a characteristic feature; namely, the C-terminal amino acid residue flanking the cysteine residue immediately downstream of the signal peptide is threonine, although the corresponding amino acid of common bacterial lipoproteins is glycine, alanine, or serine.

To analyze the pathological roles of this paralogous lipoprotein group, we attempted to synthesize a lipopeptide having an N-terminal sequence common to these lipoproteins. The results of previous work suggested that synthetic lipopeptides with original peptide sequences with more than 10 amino acids could mimic the immunostimulatory activity of natural lipoproteins (24, 27, 32). Therefore, we determined that the partial consensus sequence of MPN271, MPN369, MPN411, MPN467, and MPN654 is TGIQADLRNLIK, which should couple to an *S*-dipalmitoylglyceryl cysteine. The structure was chemically synthesized using a method similar to the method used for synthesis of known mycoplasmal lipopeptides described previously (17, 32), and the protein was designated MPPL-1 (Fig. 1B). All of our preparations of mycoplasmal lipopeptides were synthesized as mixtures of the *S*-form and *R*-form stereoisomers.

Immunostimulatory activity of MPPL-1. To investigate the immunostimulatory activity of MPPL-1, we examined the induction of cytokine production in human monocytic THP-1 cells, comparing the activity of MPPL-1 with the activities of two synthetic mycoplasmal lipopeptides. MALP-2 (*S*-dipalmitoylglyceryl CGNNDESNISFKEK) derived from *Mycoplasma fermentans* was first identified and characterized by Mühlradt's group as a compound that can activate macrophages even at picomolar concentrations (24). FSL-1 (*S*-dipalmitoylglyceryl CGDPKHPKSF) derived from *Mycoplasma salivarium* has recently been characterized by our group as a potent immunostimulatory compound, whose activity has been proposed to be stronger than that of MALP-2 (16, 17, 27). MPPL-1 could induce production of IL-8 in a dose-dependent manner at a concentration of ≥10 nM, whereas FSL-1 and MALP-2 could induce the production of IL-8 at picomolar concentrations (Fig. 2A). To induce a level of IL-8 production similar to the level induced by 1 nM FSL-1, a 300-fold-higher concentration of MPPL-1 was required (Fig. 2A). Moreover, similar weak activity of MPPL-1 was also observed when IL-6 production in THP-1 cells was examined (Fig. 2B). In this case, the concentration of FSL-1 needed to induce a level of IL-6 production similar to that induced by 1 μM MPPL-1 was 700-fold lower (Fig. 2B). Thus, the immunostimulatory activity of MPPL-1 is much weaker than the activities of structurally similar lipopeptides.

TLR recognition of MPPL-1. It has been shown that FSL-1 and MALP-2 stimulate human cells via recognition by TLR2 and TLR6 (26, 27, 35). We first examined whether MPPL-1 was recognized by TLR2 using HEK293 cells intrinsically lacking expression of TLR2 and responsiveness to TLR2 ligands (1). MPPL-1 could not stimulate parental HEK293 cells at concentrations ranging from 100 fM to ~10 μM (data not shown) but could stimulate the cells stably transfected with TLR2, leading to induction of NF-κB activation, in a dose-dependent manner (Fig. 3A). Therefore, MPPL-1 recognition was completely dependent on TLR2 in the same way that FSL-1 and MALP-2 recognition was. However, an approximately 1,000-fold-higher concentration of MPPL-1 was re-

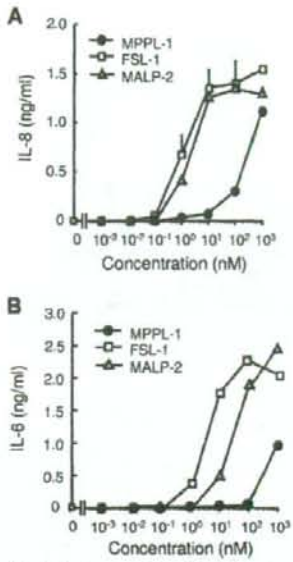

FIG. 2. Cytokine-inducing activity of MPPL-1. A total of 1×10^5 THP-1 cells were stimulated for 12 h with the concentrations of MPPL-1, FSL-1, and MALP-2 indicated. Then the amounts of IL-8 (A) and IL-6 (B) released into the media were determined by ELISA. The results are representative of three separate experiments, and the data are means and standard deviations.

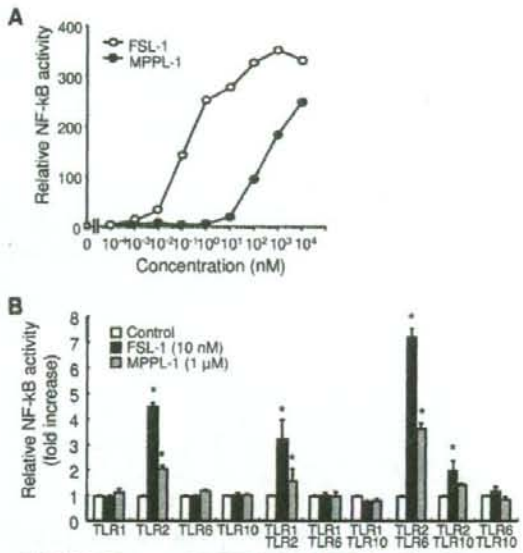

FIG. 3. TLR usage of MPPL-1. (A) HEK293 cells stably transfected with TLR2 were prepared and transiently transfected with an NF-κB-driven firefly luciferase reporter plasmid. The cells were stimulated for 6 h with the concentrations of MPPL-1 and FSL-1 indicated. Then the cells were lysed, and the luciferase activity was measured. The results, expressed as the means of values for triplicate wells, are representative of three separate experiments. (B) HEK293 cells were transiently transfected with an NF-κB-driven firefly luciferase reporter plasmid together with the TLR-encoding plasmids indicated. The cells were stimulated for 6 h with 1 μM MPPL-1 or 10 nM FSL-1. Then the cells were lysed, and the luciferase activity was measured. The results, expressed as means and standard deviations of values for triplicate wells, are representative of three separate experiments. An asterisk indicates that the P value was <0.05 for a comparison with the control group.

quired for activity similar to that of FSL-1 in TLR2-expressing HEK293 cells (Fig. 3A).

We further investigated the requirement for TLR1, TLR6, and TLR10 for recognition of MPPL-1, since TLR2 has been shown to form not only a homomer but also heteromers with these TLRs (29). MPPL-1 could not activate HEK293 cells transfected with TLR1, TLR6, or TLR10 alone (Fig. 3B). Similarly, MPPL-1 could not activate cells transfected with a combination of TLR1 and TLR6, TLR1 and TLR10, or TLR6 and TLR10 (Fig. 3B). Compared with the MPPL-1 activity in the cells transfected with TLR2 alone, cotransfection of TLR6 with TLR2 synergically augmented the activity of MPPL-1 in a way similar to way observed with FSL-1, whereas cotransfection of TLR1 or TLR10 with TLR2 did not (Fig. 3B). Thus, MPPL-1 is preferentially recognized by TLR2/TLR6 in human cells in a manner similar to the recognition of FSL-1 and MALP-2.

Possibility of an antagonistic effect of MPPL-1 on TLR2 recognition. TLR4 recognition of *E. coli* lipopolysaccharide can be antagonized by structurally similar compounds that have weak TLR4-stimulating activities (9, 10, 23, 25). However, it is still not clear whether TLR2 recognition of lipopeptides can be antagonized by structurally similar compounds. The results described above raise the possibility that MPPL-1 has an antagonistic effect on FSL-1 recognition by TLR2/TLR6, because MPPL-1 exhibits a much lower level of activity than FSL-1 exhibits through recognition by TLR2/TLR6. We therefore examined the IL-6-producing activity of FSL-1 in the presence and absence of a higher concentration of MPPL-1. IL-6 production induced by 1 or 10 nM FSL-1 was not altered by the presence of 1 μM MPPL-1 (Fig. 4A). Moreover, the presence of MPPL-1 was found to slightly increase the activity of FSL-1 as determined by analysis of NF-κB activation in HEK293 cells (Fig. 4B), and this analysis was more sensitive than an IL-6 ELISA with THP-1 cells. In addition, the MPPL-1 effect on FSL-1 recognition was not altered in the presence or absence of TLR1, TLR6, or TLR10 cotransfection (Fig. 4B). Similar results were obtained in experiments using MALP-2 (data not shown).

DISCUSSION

We have been interested in the immunostimulatory activity of mycoplasmal diacylated lipoproteins/lipopeptides and the pathological roles of these proteins in mycoplasmal infections. So far, lipopeptides FSL-1 and MALP-2 have been identified as potent immunostimulatory compounds (22, 24). In this study, we synthesized lipopeptide MPPL-1 having a structure common in mycoplasmal lipopeptides, an *S*-dipalmitoylglyceryl cysteine residue coupled to a distinct peptide, which was determined on the basis of paralogous lipoproteins charac-

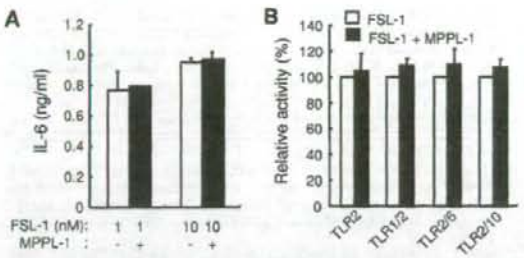

FIG. 4. Antagonistic effect of MPPL-1. (A) A total of 1×10^5 THP-1 cells were stimulated for 12 h with 1 or 10 nM FSL-1 in the presence or absence of 1 μM MPPL-1. Then the amounts of IL-6 released into the media were determined by ELISA. The results, expressed as means and standard deviations, are representative of three separate experiments. (B) HEK293 cells were transiently transfected with an NF-κB-driven firefly luciferase reporter plasmid together with the TLR-encoding plasmids indicated. The cells were stimulated for 6 h with 1 nM FSL-1 in the presence or absence of 100 nM MPPL-1. Then the cells were lysed, and the luciferase activity was measured. The results, expressed as means and standard deviations of values for triplicate wells, are representative of three separate experiments.

teristic of *M. pneumoniae*. The cytokine-inducing activity of MPPL-1 in human cells was very weak compared with that of FSL-1 or MALP-2. At a higher concentration, MPPL-1 could weakly stimulate cells via TLR2/TLR6 recognition. However, MPPL-1 could not antagonize FSL-1 recognition by TLR2. These findings raised several important possibilities for biological activities of mycopalsmal lipopeptides, as discussed below.

Recent studies have revealed that the immunostimulatory activity of bacterial lipoproteins is completely dependent on the recognition and signal transduction by TLR2 that functions together with several associated molecules. TLR6 has been considered to be an essential participant in the discrimination of mycoplasmal diacylated lipoproteins/lipopeptides by TLR2, because MALP-2 recognition was impaired in macrophages from TLR6-deficient mice (36) and was reduced by a blocking antibody to TLR6 in human cells (26). However, Buwitt-Beckmann et al. found that C-terminal addition of SKKKK to the peptide moiety of MALP-2 converted the MALP-2 recognition by TLR2/TLR6 into recognition by a TLR6-independent mechanism (6). In addition, we previously reported that substitution of the C-terminal amino acid of FSL-1 (F to R) greatly impaired the immunostimulatory activity (27). Therefore, discrimination of diacylated lipopeptides by TLR2 and TLR6 has been suggested to be dependent on the amino acid sequence or structure of the peptide portion, although recognition of the lipolyated cysteine residue may be dependent on other molecules, such as CD36 (15). Furthermore, a recent report suggested that TLR1 participates in the recognition of a dipalmitoylated lipoprotein derived from *M. pneumoniae* (MPN602) (33). In this study, MPPL-1 was shown to be recognized by TLR2 and TLR6 but not by TLR1 or TLR10, as observed for MALP-2 and FSL-1. We could not discern a role for TLR10 in the recognition of mycoplasmal lipopeptides, although it is possible that TLR10 participates in accurate discrimination of bacterial lipoproteins/lipopeptides in human cells.

It is possible that studies of TLR antagonists may lead to the development of efficient therapeutic regulators of microbial infection or excess inflammation. In this study, however, MPPL-1 could not antagonize TLR2 recognition of FSL-1 (Fig. 4). The weak TLR2-stimulating activity of MPPL-1 raises the possibility that the peptide moiety of MPPL-1 has a low affinity for TLR6 but does not have an affinity for either TLR1 or TLR10. This possibility may be supported by our results showing that a small amount of FSL-1, which may have a stronger affinity than MPPL-1 has, could be preferentially recognized by TLR2 and TLR6 more than a larger amount of MPPL-1 could be recognized (Fig. 4). Moreover, our results may provide strong evidence for different ligand recognition mechanisms of TLR2 and TLR4, because TLR4 recognition of lipopolysaccharide is known to be antagonized by structurally similar compounds that have weak TLR4-stimulating activities (9, 10, 23, 25). Further study is needed to determine the detailed recognition machinery of mycoplasmal lipoproteins/lipopeptides.

The magnitude of the immunostimulatory activity of bacterial lipoproteins has been thought to be one of the crucial factors for pathogenicity of bacteria (3) which may be involved in the severity of host immune responses after bacterial infection. However, the presence of immunostimulatory compounds on the surface of bacterial cells leads to efficient clearance of bacteria through activation of immune cells, resulting in great reductions in efficient propagation and colonization on the host cell surface. To avoid activation of immune responses, several pathogenic bacteria have been shown to modify their surface molecules so they do not stimulate the TLR recognition system. For example, α- and ε-*Proteobacteria*, including *Campylobacter jejuni*, *Helicobacter pylori*, and *Bartonella bacilliformis*, modify the N-terminal D1 domain of flagellin, leading to evasion of TLR5 recognition (2). Therefore, structural modification of pathogen-activated molecular patterns may be important for bacterial pathogenicity. However, it has not been determined whether *M. pneumoniae* has the ability to evade immune systems. So far, mycoplasmal lipoproteins/lipopeptides have been identified to determine strong activators of immune cells in crude mixtures of lipoproteins obtained using methods such as Triton X-114 phase separation (24, 32, 33). In a recent study performed by Shimizu et al. (33), lipoprotein MPN602, which may have the strongest activities in *M. pneumoniae* lipoprotein mixtures, was identified by using a method to separate the fraction that strongly stimulates 293T cells transfected with TLR2 to activate NF-κB (33). MPN602 does not belong to a paralogous lipoprotein family, as shown in Table S1 in the supplemental material. Interestingly, it was also found that only a few lipoproteins possessed strong immunostimulatory activities and that the majority of lipoproteins had weak or no immunostimulatory activity (24, 32, 33). Consistent with this possibility, only a few lipoproteins with potent immunostimulatory activity have been identified so far, although there are many lipoproteins in mycoplasmal species. These observations suggest that the majority of lipoproteins of *M. pneumoniae*, including paralogous lipoprotein family members, have weak immunostimulatory activities. Moreover, our results suggest that propagation of genes encoding lipoproteins with

weak immunostimulatory activity may be an important factor for the pathogenicity of *M. pneumoniae* through which the microorganism may evade TLR2 recognition. Further detailed investigations of the functions and immunostimulatory activities of lipoproteins found in *M. pneumoniae* are needed to address this possibility.

The bacterial lipoprotein structure has been found to be a lipidated (commonly palmitoylated) triacylated or diacylated *S*-glyceryl cysteine residue coupled to distinct polypeptides. However, the coupled peptide sequence has been shown to have a great effect on the immunostimulatory activity of the whole molecule. Therefore, synthesis and characterization of lipopeptides based on the known lipoprotein sequences of the N terminus may be an effective method for determining unknown biological activities of bacterial lipoproteins. Moreover, exhaustive screening of synthetic lipopeptides can lead to the identification of novel bacterial pathogenicities and to the development of biologically beneficial compounds or immune regulators. Also, it is possible that a cognate ligand for TLR10 will be identified by screening of these lipopeptides.

ACKNOWLEDGMENTS

This work was supported by grants-in-aid for young scientists (B): 16791102 and (B):18791363 to T.I. provided by the Ministry of Education, Culture, Sports, Science and Technology, Japan.

REFERENCES

1. **Aliprantis, A. O., R. B. Yang, M. R. Mark, S. Suggett, B. Devaux, J. D. Radolf, G. R. Klimpel, P. Godowski, and A. Zychlinsky.** 1999. Cell activation and apoptosis by bacterial lipoproteins through Toll-like receptor-2. Science **285:**736–739.
2. **Andersen-Nissen, E., K. D. Smith, K. L. Strobe, S. L. Barrett, B. T. Cookson, S. M. Logan, and A. Aderem.** 2005. Evasion of Toll-like receptor 5 by flagellated bacteria. Proc. Natl. Acad. Sci. USA **102:**9247–9252.
3. **Brightbill, H. D., D. H. Libraty, S. R. Krutzik, R. B. Yang, J. T. Belisle, J. R. Bleharski, M. Maitland, M. V. Norgard, S. E. Plevy, S. T. Smale, P. J. Brennan, B. R. Bloom, P. J. Godowski, and R. L. Modlin.** 1999. Host defense mechanisms triggered by microbial lipoproteins through Toll-like receptors. Science **285:**732–736.
4. **Bulut, Y., E. Faure, L. Thomas, O. Equils, and M. Arditi.** 2001. Cooperation of Toll-like receptor 2 and 6 for cellular activation by soluble tuberculosis factor and *Borrelia burgdorferi* outer surface protein A lipoprotein: role of Toll-interacting protein and IL-1 receptor signaling molecules in Toll-like receptor 2 signaling. J. Immunol. **167:**987–994.
5. **Buwitt-Beckmann, U., H. Heine, K. H. Wiesmuller, G. Jung, R. Brock, S. Akira, and A. J. Ulmer.** 2006. TLR1- and TLR6-independent recognition of bacterial lipopeptides. J. Biol. Chem. **281:**9049–9057.
6. **Buwitt-Beckmann, U., H. Heine, K. H. Wiesmuller, G. Jung, R. Brock, S. Akira, and A. J. Ulmer.** 2005. Toll-like receptor 6-independent signaling by diacylated lipopeptides. Eur. J. Immunol. **35:**282–289.
7. **Chambaud, I., H. Wroblewski, and A. Blanchard.** 1999. Interactions between mycoplasma lipoproteins and the host immune system. Trends Microbiol. **7:**493–499.
8. **Chuang, T., and R. J. Ulevitch.** 2001. Identification of hTLR10: a novel human Toll-like receptor preferentially expressed in immune cells. Biochim. Biophys. Acta **1518:**157–161.
9. **Coats, S. R., T. T. Pham, B. W. Bainbridge, R. A. Reife, and R. P. Darveau.** 2005. MD-2 mediates the ability of tetra-acylated and penta-acylated lipopolysaccharides to antagonize *Escherichia coli* lipopolysaccharide at the TLR4 signaling complex. J. Immunol. **175:**4490–4498.
10. **Coats, S. R., R. A. Reife, B. W. Bainbridge, T. T. Pham, and R. P. Darveau.** 2003. *Porphyromonas gingivalis* lipopolysaccharide antagonizes *Escherichia coli* lipopolysaccharide at Toll-like receptor 4 in human endothelial cells. Infect. Immun. **71:**6799–6807.
11. **Hallamaa, K. M., G. F. Browning, and S. L. Tang.** 2006. Lipoprotein multigene families in *Mycoplasma pneumoniae*. J. Bacteriol. **188:**5393–5399.
12. **Hasan, U., C. Chaffois, C. Gaillard, V. Saulnier, E. Merck, S. Tancredi, C. Guiet, F. Briere, J. Vlach, S. Lebecque, G. Trinchieri, and E. E. Bates.** 2005. Human TLR10 is a functional receptor, expressed by B cells and plasmacytoid dendritic cells, which activates gene transcription through MyD88. J. Immunol. **174:**2942–2950.
13. **Himmelreich, R., H. Hilbert, H. Plagens, E. Pirkl, B. C. Li, and R. Herrmann.** 1996. Complete sequence analysis of the genome of the bacterium *Mycoplasma pneumoniae*. Nucleic Acids Res. **24:**4420–4449.
14. **Himmelreich, R., H. Plagens, H. Hilbert, B. Reiner, and R. Herrmann.** 1997. Comparative analysis of the genomes of the bacteria *Mycoplasma pneumoniae* and *Mycoplasma genitalium*. Nucleic Acids Res. **25:**701–712.
15. **Hoebe, K., P. Georgel, S. Rutschmann, X. Du, S. Mudd, K. Crozat, S. Sovath, L. Shamel, T. Hartung, U. Zahringer, and B. Beutler.** 2005. CD36 is a sensor of diacylglycerides. Nature **433:**523–527.
16. **Hubschle, T., J. Mutze, P. F. Muhlradt, S. Korte, R. Gerstberger, and J. Roth.** 2006. Pyrexia, anorexia, adipsia, and depressed motor activity in rats during systemic inflammation induced by the Toll-like receptors-2 and −6 agonists MALP-2 and FSL-1. Am. J. Physiol. Regul. Integr. Comp. Physiol. **290:**R180–187.
17. **Into, T., M. Fujita, T. Okusawa, A. Hasebe, M. Morita, and K. Shibata.** 2002. Synergic effects of mycoplasmal lipopeptides and extracellular ATP on activation of macrophages. Infect. Immun. **70:**3586–3591.
18. **Into, T., K. Kiura, M. Yasuda, H. Kataoka, N. Inoue, A. Hasebe, K. Takeda, S. Akira, and K. Shibata.** 2004. Stimulation of human Toll-like receptor (TLR) 2 and TLR6 with membrane lipoproteins of *Mycoplasma fermentans* induces apoptotic cell death after NF-κB activation. Cell. Microbiol. **6:**187–199.
19. **Into, T., Y. Nodasaka, A. Hasebe, T. Okuzawa, J. Nakamura, N. Ohata, and K. Shibata.** 2002. Mycoplasmal lipoproteins induce Toll-like receptor 2- and caspases-mediated cell death in lymphocytes and monocytes. Microbiol. Immunol. **46:**265–276.
20. **Into, T., and K. Shibata.** 2005. Apoptosis signal-regulating kinase 1-mediated sustained p38 mitogen-activated protein kinase activation regulates mycoplasmal lipoprotein- and staphylococcal peptidoglycan-triggered Toll-like receptor 2 signalling pathways. Cell. Microbiol. **7:**1305–1317.
21. **Kirschning, C. J., and R. R. Schumann.** 2002. TLR2: cellular sensor for microbial and endogenous molecular patterns. Curr. Top. Microbiol. Immunol. **270:**121–144.
22. **Kiura, K., H. Kataoka, T. Nakata, T. Into, M. Yasuda, S. Akira, N. Inoue, and K. Shibata.** 2006. The synthetic analogue of mycoplasmal lipoprotein FSL-1 induces dendritic cell maturation through Toll-like receptor 2. FEMS Immunol. Med. Microbiol. **46:**78–84.
23. **Lepper, P. M., M. Triantafilou, C. Schumann, E. M. Schneider, and K. Triantafilou.** 2005. Lipopolysaccharides from *Helicobacter pylori* can act as antagonists for Toll-like receptor 4. Cell. Microbiol. **7:**519–528.
24. **Mühlradt, P. F., M. Kiess, H. Meyer, R. Sussmuth, and G. Jung.** 1997. Isolation, structure elucidation, and synthesis of a macrophage stimulatory lipopeptide from *Mycoplasma fermentans* acting at picomolar concentration. J. Exp. Med. **185:**1951–1958.
25. **Mullarkey, M., J. R. Rose, J. Bristol, T. Kawata, A. Kimura, S. Kobayashi, M. Przetak, J. Chow, F. Gusovsky, W. J. Christ, and D. P. Rossignol.** 2003. Inhibition of endotoxin response by e5564, a novel Toll-like receptor 4-directed endotoxin antagonist. J. Pharmacol. Exp. Ther. **304:**1093–1102.
26. **Nakao, Y., K. Funami, S. Kikkawa, M. Taniguchi, M. Nishiguchi, Y. Fukumori, T. Seya, and M. Matsumoto.** 2005. Surface-expressed TLR6 participates in the recognition of diacylated lipopeptide and peptidoglycan in human cells. J. Immunol. **174:**1566–1573.
27. **Okusawa, T., M. Fujita, J. Nakamura, T. Into, M. Yasuda, A. Yoshimura, Y. Hara, A. Hasebe, D. T. Golenbock, M. Morita, Y. Kuroki, T. Ogawa, and K. Shibata.** 2004. Relationship between structures and biological activities of mycoplasmal diacylated lipopeptides and their recognition by Toll-like receptors 2 and 6. Infect. Immun. **72:**1657–1665.
28. **Omueti, K. O., J. M. Beyer, C. M. Johnson, E. A. Lyle, and R. I. Tapping.** 2005. Domain exchange between human Toll-like receptors 1 and 6 reveals a region required for lipopeptide discrimination. J. Biol. Chem. **280:**36616–36625.
29. **Ozinsky, A., D. M. Underhill, J. D. Fontenot, A. M. Hajjar, K. D. Smith, C. B. Wilson, L. Schroeder, and A. Aderem.** 2000. The repertoire for pattern recognition of pathogens by the innate immune system is defined by cooperation between Toll-like receptors. Proc. Natl. Acad. Sci. USA **97:**13766–13771.
30. **Rawadi, G.** 2000. *Mycoplasma fermentans* interaction with monocytes/macrophages: molecular basis. Microbes Infect. **2:**955–964.
31. **Rottem, S.** 2003. Interaction of mycoplasmas with host cells. Physiol. Rev. **83:**417–432.
32. **Shibata, K., A. Hasebe, T. Into, M. Yamada, and T. Watanabe.** 2000. The N-terminal lipopeptide of a 44-kDa membrane-bound lipoprotein of *Mycoplasma salivarium* is responsible for the expression of intercellular adhesion molecule-1 on the cell surface of normal human gingival fibroblasts. J. Immunol. **165:**6538–6544.
33. **Shimizu, T., Y. Kida, and K. Kuwano.** 2005. A dipalmitoylated lipoprotein from *Mycoplasma pneumoniae* activates NF-κB through TLR1, TLR2, and TLR6. J. Immunol. **175:**4641–4646.
34. **Takeda, K., T. Kaisho, and S. Akira.** 2003. Toll-like receptors. Annu. Rev. Immunol. **21:**335–376.
35. **Takeuchi, O., A. Kaufmann, K. Grote, T. Kawai, K. Hoshino, M. Morr, P. F. Muhlradt, and S. Akira.** 2000. Preferentially the *R*-stereoisomer of the mycoplasmal lipopeptide macrophage-activating lipopeptide-2 activates im-

mune cells through a Toll-like receptor 2- and MyD88-dependent signaling pathway. J. Immunol. **164:**554–557.
36. **Takeuchi, O., T. Kawai, P. F. Muhlradt, M. Morr, J. D. Radolf, A. Zychlinsky, K. Takeda, and S. Akira.** 2001. Discrimination of bacterial lipoproteins by Toll-like receptor 6. Int. Immunol. **13:**933–940.
37. **Takeuchi, O., S. Sato, T. Horiuchi, K. Hoshino, K. Takeda, Z. Dong, R. L. Modlin, and S. Akira.** 2002. Role of Toll-like receptor 1 in mediating immune response to microbial lipoproteins. J. Immunol. **169:**10–14.
38. **Waites, K. B., and D. F. Talkington.** 2004. *Mycoplasma pneumoniae* and its role as a human pathogen. Clin. Microbiol. Rev. **17:**697–728.
39. **Weiner, J., 3rd, R. Herrmann, and G. F. Browning.** 2000. Transcription in *Mycoplasma pneumoniae*. Nucleic Acids Res. **28:**4488–4496.

Editor: D. L. Burns

MOLECULAR AND CELLULAR BIOLOGY, Feb. 2008, p. 1338–1347 Vol. 28, No. 4
0270-7306/08/$08.00+0 doi:10.1128/MCB.01412-07

Regulation of MyD88-Dependent Signaling Events by S Nitrosylation Retards Toll-Like Receptor Signal Transduction and Initiation of Acute-Phase Immune Responses▽

Takeshi Into,[1]* Megumi Inomata,[1] Misako Nakashima,[1] Ken-ichiro Shibata,[2] Hans Häcker,[3] and Kenji Matsushita[1]

Department of Oral Disease Research, National Institute for Longevity Sciences, National Center for Geriatrics and Gerontology, 36-3, Gengo, Morioka, Obu, Aichi 474-8522, Japan[1]; Laboratory of Oral Molecular Microbiology, Department of Oral Pathobiological Science, Hokkaido University Graduate School of Dental Medicine, Sapporo 060-8586, Japan[2]; and Department of Infectious Diseases, St. Jude Children's Research Hospital, 332 North Lauderdale Street, Memphis, Tennessee 38105[3]

Received 7 August 2007/Returned for modification 23 September 2007/Accepted 28 November 2007

Nitric oxide (NO) has been thought to regulate the immune system through S nitrosylation of the transcriptional factor NF-κB. However, regulatory effects of NO on innate immune responses are unclear. Here, we report that NO has a capability to control Toll-like receptor-mediated signaling through S nitrosylation. We found that the adaptor protein MyD88 was primarily S nitrosylated, depending on the presence of endothelial NO synthase (eNOS). S nitrosylation at a particular cysteine residue within the TIR domain of MyD88 resulted in slight reduction of the NF-κB-activating property. This modification could be restored by the antioxidant glutathione. Through S nitrosylation, NO could negatively regulate the multiple steps of MyD88 functioning, including translocation to the cell membrane after LPS stimulation, interaction with TIRAP, binding to TRAF6, and induction of IκBα phosphorylation. Interestingly, glutathione could reversely neutralize such NO-derived effects. We also found that an acute febrile response to LPS was precipitated in eNOS-deficient mice, indicating that eNOS-derived NO exerts an initial suppressive effect on inflammatory processes. Thus, NO has a potential to retard induction of MyD88-dependent signaling events through the reversible and oxidative modification by NO, by which precipitous signaling reactions are relieved. Such an effect may reflect appropriate regulation of the acute-phase inflammatory responses in living organisms.

It is increasingly becoming evident that nitric oxide (NO) regulates a broad spectrum of protein functions through S nitrosylation, a posttranscriptional modification that forms *S*-nitrosothiol by covalent addition to cysteine residues of an NO moiety (14, 42, 43). Through S nitrosylation, NO is thought to exert a physiological inhibitory effect on nuclear factor κB (NF-κB) (25, 32, 33, 39), the major transcriptional factor family deeply associated with regulation of the immune system through transcription of a wide range of genes, including cytokines, adhesion molecules, antimicrobial molecules, and antiapoptotic molecules (10, 13, 24). S nitrosylation of NF-κB inhibits its DNA binding, promoter activity, and subsequent transcription (25, 33). It has been known that S nitrosylation targets a particular cysteine residue of the NF-κB p50 and p65 subunits located in the N-terminal DNA binding loop within the Rel homology domain (25, 32, 33). This residue is conserved in other NF-κB subunits, including p52, p100, p105, and c-Rel, and other Rel homology domain-containing molecules. Upstream of NF-κB, IκB kinase β (IKKβ), a catalytic subunit of the IκB (inhibitor of NF-κB) kinase complex, also undergoes S nitrosylation, resulting in reduction of its kinase function on phosphorylation of IκB (39). Such reduction of the IKKβ function leads to reduced IκB ubiquitinylation and proteasomal degradation, resulting in NF-κB inhibition (14, 32, 39).

Toll-like receptors (TLRs) are the central innate immune sensors for a broad array of pathogen-associated molecular patterns, ranging from bacterial constituents to viral genomes (2, 35). TLRs initiate early processes of proinflammatory immune responses that help to strengthen the processes of innate and adaptive immunity (2, 20), in which NF-κB plays many important roles (13, 24). TLRs utilize MyD88, a Toll/interleukin-1 receptor (IL-1R) homology (TIR) domain-containing adaptor molecule, to activate the NF-κB pathway through IL-1R-associated kinases (IRAKs) and tumor necrosis factor (TNF) receptor-associated factor 6 (TRAF6) (1). It has been thought that TLR agonistic molecules, such as lipopolysaccharide (LPS), can regulate NO generation through upregulation of expression of all NO synthase (NOS) isoforms through NF-κB activation (4, 9, 32). TLR stimulation can directly activate an antimicrobial property through inducible NOS (iNOS) expression and NO generation in macrophages (46). NO generation is a general feature of immune cells, including neutrophils, monocytes, macrophages, dendritic cells, and NK cells, as well as other cells, including endothelial cells, epithelial cells, and fibroblasts (4), all of which express multiple members of the TLR family. However, it has remained obscure whether generated NO exerts any regulatory effects on TLR signaling or subsequent processes of innate immune responses.

There has been an accumulation of biochemical evidence indicating that TLR signaling components, including IKKβ

* Corresponding author. Mailing address: Section of Oral Infection Control, Department of Oral Disease Research, National Institute for Longevity Sciences, National Center for Geriatrics and Gerontology, 36-3 Gengo, Morioka, Obu, Aichi 474-8522, Japan. Phone: 81-562-44-5651, ext. 5064. Fax: 81-562-46-8684. E-mail: into@nils.go.jp.

▽ Published ahead of print on 17 December 2007.

and NF-κB, might be regulated by S nitrosylation. S nitrosylation inhibits the kinase activity of apoptosis signal regulation kinase 1 (ASK1) through inhibition of its binding to substrates (38). ASK1 is known as an important regulator of the TRAF6-p38 mitogen-activated protein kinase (MAPK) pathway downstream of TLR4 and is also involved in modulation of both the NF-κB and apoptotic pathways downstream of TLR2 (19, 34). Caspse-1 was recently found to be involved in TLR2- and TLR4-mediated signal transduction of the MyD88-dependent pathway through the cleavage of the TIR domain-containing adaptor protein TIRAP (also known as Mal) (37). Caspase-1 also undergoes S nitrosylation at a cysteine residue within the enzymatic active site, suppressing its proteolytic activity (6, 31). Thus, it is possible that NO provides regulatory effects on the multiple steps of TLR-mediated innate immune signaling through S nitrosylation. In this study, we therefore designed experiments to determine the effect of S nitrosylation on TLR signaling. We further investigated how S nitrosylation affects TLR-initiated immune responses in vivo. We report here that S nitrosylation controls TLR signaling through redox-sensitive and reversible suppression of the MyD88 pathway, which facilitates appropriate control of acute-phase inflammatory responses in vivo.

MATERIALS AND METHODS

Reagents and cell culture. N^G-Monomethyl-L-arginine monoacetate (L-NMMA), *S*-nitrosoglutathione (GSNO), glutathione (GSH), *N*-ethylmaleimide, coumermycin A, *N*-acetyl L-cysteine (NAC), ascorbic acid, and diphenyleneiodonium (DPI) were obtained from Sigma-Aldrich. SNAP (5-nitroso-*N*-acetyl-D,L-penicillamine) was purchased from Cayman Chemical. ODQ (1*H*-[1,2,4]oxadiazolo[4,3-*a*]quinoxalin-1-one) and KT5823 were obtained from Calbiochem. Preparation of TLR ligands, including highly purified *Escherichia coli* LPS, *Salmonella* LPS, Pam_3CSK_4, macrophage-activating lipopeptide 2 (MALP-2), and *Salmonella enterica* serovar Typhimurium flagellin, was as described previously (18). Recombinant human IL-1β was from R&D Systems. Human aortic endothelial cells (HAECs) and human embryonic kidney 293 (HEK293) cells were maintained as described previously (18). HEK293 cells stably expressing human TLR4, MD2, and CD14 (293-TLR4 cells) and HEK293 cells stably expressing human TLR2 and CD14 (293-TLR2 cells) were obtained from InvivoGen.

Mice. iNOS-deficient ($iNOS^{-/-}$) mice and endothelial-NOS (eNOS)-deficient ($eNOS^{-/-}$) mice were from The Jackson Laboratories. C57BL/6J control (wild-type) mice were obtained from Japan SLC. All mice were kept under specific pathogen-free conditions. Male mice between 6 and 10 weeks of age were used for all of experiments. All animal protocols were approved by the National Institute for Longevity Sciences Animal Experimentation Committee at the National Center for Geriatrics and Gerontology (Aichi, Japan).

For LPS-induced acute lung injury, anesthetized mice received *Escherichia coli* LPS dissolved in pyrogen-free phosphate-buffered saline (PBS) containing 1 mg/ml Evans Blue intratracheally immediately after mechanical ventilation. After 30 min of administration, lung was excised and then lysed for immunoblot analysis. The febrile responses in mice treated with *E. coli* LPS were tested according to a protocol described previously (45, 49). Mice ($n = 6$) were maintained at a neutral ambient temperature of 31°C and challenged by intraperitoneal (i.p.) injection of 5 mg LPS/kg of body weight dissolved in pyrogen-free PBS. A high dose of LPS (more than 50 mg/kg) was fatal within 90 min in $eNOS^{-/-}$ mice. A colonic thermocouple was inserted and fixed to the base of the tail with adhesive tape. The change in temperature was monitored at 5-min intervals during a period of 120 min after LPS administration. All of the tests were performed at the temperature of 31°C. After 2 h or 12 h of LPS administration, 2 ml of PBS was injected into the abdominal cavity of each mouse. Then, fluids were collected and centrifuged for assessment of cytokine production by an enzyme-linked immunosorbent assay (ELISA). Preparation of peritoneal macrophages was as described previously (28).

Plasmids. The DNA construct encoding 3× Flag-tagged MyD88 fused to the B subunit of the bacterial DNA gyrase (MyD88-GyrB) was as described previously (11). Plasmids encoding human MyD88 and TIRAP were kind gifts from Margaret K. Offermann (Emory University School of Medicine). The cDNAs of N-terminal Flag-tagged and Myc-tagged MyD88, Myc-tagged TIRAP, and IRAK-1 were amplified by PCR and cloned into the pcDNA3.1 vector (Invitrogen). The construct encoding human TLR2 was as described previously (17). Constructs encoding mutated Flag-MyD88 were obtained using a QuikChange II site-directed mutagenesis kit (Stratagene) according to the manufacturer's instructions.

Protein purification. Recombinant Flag-MyD88 proteins were prepared using a FLAG M purification kit (Sigma-Aldrich) from HEK293 cells stably expressing Flag-MyD88 constructs, according to the manufacturer's instructions. Purity of recombinant proteins was confirmed by sodium dodecyl sulfate-polyacrylamide gel electrophoresis (SDS-PAGE), followed by silver staining and immunoblotting with anti-Flag antibody.

Detection of S-nitrosylated proteins. To detect S-nitrosylated MyD88 from lung lysates from wild-type mice and $eNOS^{-/-}$ mice, we referred to the protocol described by Jaffrey et al. (21). Several experiments were performed using a NitroGlo nitrosylation detection kit (PerkinElmer) according to the manufacturer's instructions. Lung lysates from wild-type and $eNOS^{-/-}$ mice were subjected to the biotin switching S-nitrosylation assay, and then biotinylated proteins were purified on streptavidin-agarose. Purified proteins eluted by 2-mercaptoethanol were detected by immunoblotting with anti-MyD88 antibody.

The quantitative measurement of S-nitrosylated recombinant MyD88 by ELISA was performed as follows. Briefly, recombinant Flag-MyD88 (150 μg) was treated with or without SNAP for 30 min at 37°C in the dark. Then, the free sulfides of Flag-MyD88 were blocked with 4 mM methylmethanethionsulfonate for 15 min. After purification by using Micro Bio-Spin chromatography columns (Bio-Rad Laboratories), Flag-MyD88 was reacted with 25 mM ascorbate to be completely denitrosylated. Free sulfides were then labeled with a biotin-conjugated maleimide, using a biotin labeling kit (SH; Dojindo Laboratories) according to the manufacturer's instructions. The diluents of biotinylated Flag-MyD88 proteins dissolved in Tris-buffered saline (pH 7.2) were stabilized in the wells of immobilizer streptavidin plates (Nunc). Flag-MyD88 proteins in the wells were detected by using anti-Flag antibody and a secondary antibody conjugated with horseradish peroxidase. Colorimetric reaction was detected by absorbance on a spectrophotometer at 450 nm. Results were expressed as means ± standard deviations (SD) of three determinations.

Photolysis of S-nitrosylated proteins. Mouse lung lysates were exposed for 3 min to a UV-visible light mercury vapor lamp according to a protocol recently described (8). The samples were then subjected to the biotin switch technique as described above.

Luciferase reporter assay. 293-TLR2 cells were transiently transfected with wild-type MyD88-GyrB or MyD88-GyrB mutants, each with a cysteine residue replaced with a serine residue, together with 50 ng of an NF-κB (3×) luciferase reporter plasmid (pNF-κB-Luc; Stratagene) and 5 ng of an internal control luciferase reporter plasmid (pRL-TK; Promega) and incubated for 16 h. At 6 h before the end of incubation, cells were treated with or without 250 μM SNAP. Cells were then stimulated with 100 ng/ml Pam_3CSK_4 for 6 h. HEK293 cells stably expressing MyD88-GyrB were transfected with pNF-κB-Luc and pRL-TK. After 24 h of incubation, cells were stimulated with coumermycin A in the presence and absence of 250 μM SNAP. The dual luciferase activity was measured as described previously (19).

Immunoblot analysis of IRAK-1 and IκBα. HAECs were stimulated with 10 ng/ml of LPS for 0 to 90 min. HEK293 cells stably expressing MyD88-GyrB were stimulated with 1 μM coumermycin for 20 min. Cells were lysed in the presence of protease inhibitor and phosphatase inhibitor cocktails (Roche) at 4°C. Cell lysates or lysates from the mouse lungs were separated by SDS-PAGE, followed by immunoblot analyses using anti-IRAK-1, anti-IκBα, and phosphorylation-specific anti-IκBα (Ser32/Ser36) antibodies (Cell Signaling Technology).

RNA extraction and reverse transcription-PCR. Total RNA was isolated from mouse peritoneal macrophages stimulated with 100 ng/ml LPS and 10 ng/ml gamma interferon, and transcripts were quantified by real-time quantitative reverse transcription-PCR on a LightCycler ST300 system (Roche). All values were normalized to the level of β-actin mRNA. The primer sets used are as follows: for mouse macrophage inflammatory protein 2 (MIP-2), 5′-ATCCAGAGCTTGAGTGTGACGC-3′ (sense) and 5′-AAGGCAAACTTTTTGACCGAA-3′ (antisense); for mouse IL-6, 5′-CCACGGCCTTCCCTAC-3′ (sense) and 5′-AGTGCATCATCGTTGTTC-3′ (antisense); and for mouse β-actin, 5′-AAATCGTGCGTGACATCAAA-3′ (sense) and 5′-AAGGAAGGCTGGAAAAGAGC-3′ (antisense).

Cytokine ELISA. Concentrations of human IL-8, mouse MIP-2, and mouse IL-6 were determined using a Cytoset ELISA kit (Biosource) according to the manufacturer's instructions.

Subcellular fractionation. Subcellular fractionation of HEK293 cells stably expressing Flag-MyD88 and 293-TLR4 cells stably expressing Flag-MyD88-GyrB

was performed using a ProteoExtract subcellular proteome extraction kit (Calbiochem) according to the manufacturer's instructions. This kit enables extraction of different subcellular fractions of the cytoplasm, plasma membrane, nuclei, and cytoskeleton from mammalian cells. 293-TLR4 cells stably expressing Flag-MyD88-GyrB were maintained in serum-free Dulbecco's modified Eagle's medium containing 5% PANEXIN H cell growth supplement (PAN Biotech GmbH) to avoid nonspecific cell activation by animal serum components. The whole-cell lysate was obtained using NuPAGE LDS sample buffer containing 2-mercaptoethanol. Each fraction was mixed with NuPAGE LDS sample buffer and boiled for 5 min, followed by SDS-PAGE and immunoblot analyses using anti-Flag (Sigma), anti-MyD88 (Santa Cruz Biotechnology), anti-IRAK-1, and anti-vimentin (BD Biosciences) antibodies.

Blue native PAGE and immunoprecipitation. HEK293 cells stably expressing Flag-MyD88 were treated with SNAP for 1 h, washed twice with PBS, and lysed with HEPES buffer (pH 7.2) containing 1% Triton X-100, 1% Nonidet-P40, and proteinase inhibitor cocktail (Roche). Cell lysates were separated by blue native PAGE according to the protocol provided by Invitrogen and then immunoblotted with anti-Flag antibody. HEK293 cells transiently transfected combinatorially with Flag-MyD88 and Myc-TIRAP or Flag-MyD88 and IRAK-1 were treated with GSNO or GSH for 1 h. HEK293 cells stably expressing 3× Flag-MyD88-GyrB were stimulated with 1 μM coumermycin A for 20 min. Cells were lysed with HEPES buffer (pH 7.2) containing 1% Triton X-100 and proteinase inhibitor cocktail (Roche). Clarified cell lysates were immunoprecipitated with anti-Flag antibody, followed by immunoblot analysis using anti-Flag, anti-Myc, and anti-TRAF6 (StressGen) antibodies. All experiments were performed at least three times, and representative results are shown.

Immunofluorescent cell staining. HAECs were fixed at −20°C with methanol, and double immunostaining was then carried out with anti-β-actin monoclonal antibody (Santa Cruz Biotechnology) and Alexa 488-conjugated immunoglobulin G secondary antibody (Invitrogen) and then with anti-MyD88 rabbit polyclonal antibody (Santa Cruz Biotechnology) and Alexa 564-conjugated immunoglobulin G secondary antibody (Invitrogen). Cell nuclei were also stained with 2.5 μg/ml of Hoechst 33342 for 30 min.

Statistical analysis. Probability (P) values were calculated by Student's t test and analysis of variance and were considered significant at 0.05 or 0.01.

RESULTS

TLR signaling components are S nitrosylated in vivo. To examine whether TLR signal components are physiologically S nitrosylated in vivo, we detected S-nitrosylated proteins in the lung lysates from wild-type and eNOS$^{-/-}$ mice by utilizing the biotin switch method (21). Interestingly, this method facilitated the detection of MyD88 as an S-nitrosylated protein (Fig. 1A). To exclude the possibility that the detection of S-nitrosylated MyD88 is an experimental artifact, we utilized the biotin switch method combined with photolysis of S nitrosylation, which has recently been reported as a useful method for confirming the specificity of S nitrosylation (8). The detectable S-nitrosylated MyD88 protein was reduced after exposure of the samples to a UV lamp (Fig. 1B), suggesting that the result is not false positive. Thus, our result at least suggests that MyD88 is potentially S nitrosylated in addition to other signaling molecules, including NF-κBs, ASK1, and caspase-1.

We further examined the details of S-nitrosylated MyD88 in vitro by utilizing a quantitative method for detecting S nitrosylation of recombinant proteins. We could detect S nitrosylation of recombinant MyD88, which increased, accompanied by an increase in the concentration of the NO donor SNAP (Fig. 1C). It has been known that S-nitrosylated proteins are reversibly denitrosylated by antioxidants or oxidoreductases, by which substantial protein functions are restored (14, 42). Indeed, the detectable S-nitrosylated MyD88 protein was reduced when the NO donor-treated protein was reacted with ascorbate, $HgCl_2$, or GSH (Fig. 1C). We further determined the site of S nitrosylation because the modification is effected toward particular cysteine residues (14). Mammalian MyD88 contains a total of nine cysteine residues: one in a short linker region and the other eight in the TIR domain (Fig. 1D). These residues are thought not to be involved in the formation of intramolecular disulfide bonds. Among vertebrates, all cysteine residues are highly conserved (data not shown). We prepared recombinant MyD88 proteins of nine individual mutants, each with one of the nine cysteine residues replaced with a serine residue. We found that the degrees of S nitrosylation of Cys113 and Cys216 were significantly reduced compared with those of wild-type MyD88 (Fig. 1E). These cysteine residues partially fulfill the predictive site of the S nitrosylation "acid-base motif" that comprises flanking acidic and basic residues (14) (Fig. 1F). Interestingly, the cysteine residue equivalent of Cys216 is conserved even in invertebrates, while others are not (data not shown). Among other TIR domain-containing adaptor molecules, only TIRAP and SIGIRR have a cysteine residue corresponding to the position of Cys216 (Fig. 1G).

To determine the requirement of cysteine residues for functioning of MyD88, we utilized MyD88 fused to the B subunit of the bacterial DNA gyrase (MyD88-GyrB). The *Streptomyces*-derived bivalent antibiotic coumermycin binds GyrB with a stoichiometry of 1:2, acting as a natural dimerizer of GyrB (7). Although overexpressed MyD88 is known to reveal TLR stimulation-independent nonspecific activation of downstream signaling through self-dimerization (11, 36), MyD88-GyrB does not reveal such nonspecific activation unless cells are exposed to TLR stimulation or coumermycin treatment (11). We prepared GyrB-fused wild-type MyD88 and MyD88 mutants, each with one of the nine cysteine residues replaced with a serine residue, and examined the NF-κB-activating properties in the TLR2 ligand Pam_3CSK_4-stimulated HEK293 cells stably expressing TLR2. None of the cysteine replacement mutants abrogated the NF-κB-activating property of MyD88 (Fig. 1H). However, the Cys216Ser mutant significantly increased the activity compared with that of wild-type MyD88 (Fig. 1H). Additionally, similar results were found in the cells treated with SNAP (Fig. 1H). Thus, it is possible that Cys216 of MyD88 mediates the suppressive effect of NO.

S nitrosylation alters MyD88-mediated signaling events. We next explored how S nitrosylation of signaling components alters TLR signaling events. To examine this in vivo, we utilized an animal model of acute lung injury induced by intratracheal administration of LPS. We investigated degradation of IRAK-1 and IκBα, hallmarks of MyD88-dependent and IKKβ-dependent signaling events, in the lungs 30 min after LPS administration. Interestingly, degradation of IRAK-1 and IκBα was apparently promoted in eNOS$^{-/-}$ mice compared with that in wild-type mice (Fig. 2A). We also examined whether NO alters degradation of IRAK-1 and IκBα in cultivated vascular endothelial cells. In HAECs, LPS induced degradation of IRAK-1 and IκBα within 30 min after stimulation (Fig. 2B). Degradation of IRAK-1 and IκBα was promoted and occurred within 15 min after stimulation when endogenous NO was predepleted by the L-arginine analog L-NMMA (Fig. 2B). In addition, IRAK-1 degradation was also promoted when confluent HAECs were maintained in culture media without the eNOS activator vascular endothelial growth factor or the phosphatidylinositol 3-kinase inhibitor LY294002 (data not shown). In contrast to these results, degradation was delayed

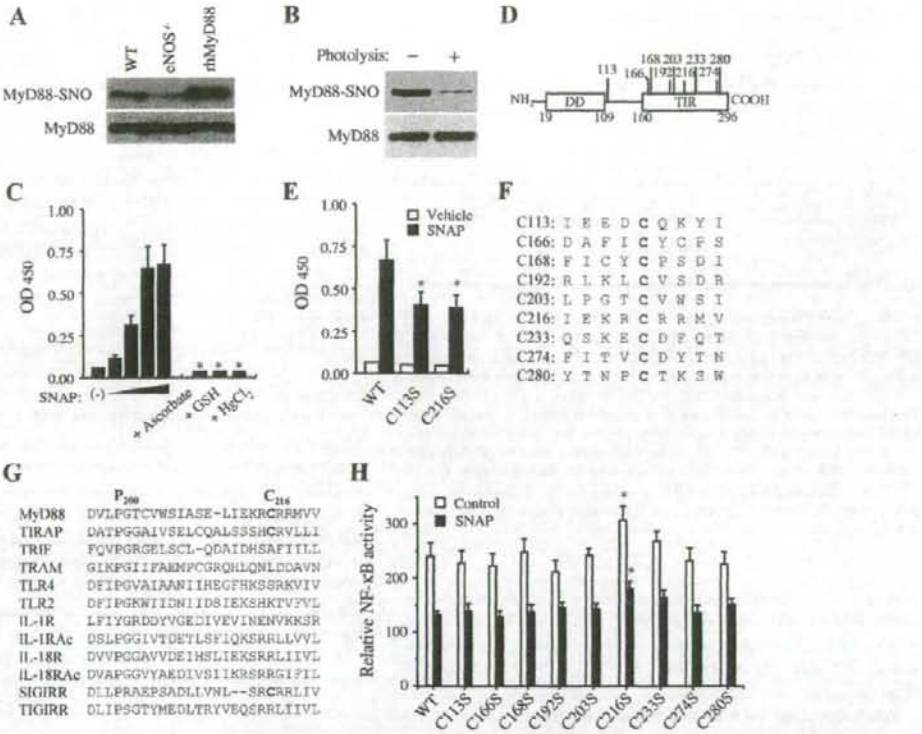

FIG. 1. S nitrosylaton of MyD88. (A) Lung lysates from wild-type (WT) and eNOS$^{-/-}$ mice and SNAP-treated recombinant human MyD88 (rhMyD88) were subjected to the biotin switching S-nitrosylation assay, and then biotinylated proteins were purified on streptavidin-agarose. Purified proteins were detected by immunoblotting with anti-MyD88 antibody (upper). MyD88 proteins in lung lysates and rhMyD88 were also shown as loading controls (lower). (B) Mouse lung lysates were exposed for 3 min to a UV-visible light mercury vapor lamp. The samples were then subjected to the biotin switch method. (C) A recombinant Flag-MyD88 protein was treated with or without SNAP (100, 200, 500, and 1,000 μM) for 30 min. For the denitrosylation study, SNAP-treated proteins were incubated with 1 mM ascorbic acid, 1 mM GSH, or 1 mM $HgCl_2$ for 5 min before the blockade of free thiols by methylmethanethionsulfonate. Then, S-nitrosylated residues of MyD88 were switched into biotins and proteins were fixed on streptavidin-coated plates, followed by ELISA with anti-Flag antibody. Each value is the mean ± SD ($n = 3$). See text for details. (*, $P < 0.01$ for comparison with the group of 500 μM SNAP). (D) Schematic of human MyD88. (E) Recombinant Flag-MyD88 wild-type proteins and mutants with each cysteine residue replaced with a serine residue were treated with or without 500 μM SNAP for 30 min. Then, S-nitrosylated MyD88 fixed on streptavidin-coated plates was detected by ELISA using anti-Flag antibody. Each value is the mean ± SD ($n = 3$). See text for details. (*, $P < 0.01$ for comparison with the wild-type group). (F) Sequence alignment of the region around nine cysteine residues of MyD88. (G) Sequence alignment of human TIR domain-containing molecules. The regions corresponding to that around the residues of Pro200, a critical residue for TIR-TIR interaction, and Cys216 of MyD88 are shown. (H) HEK293 cells stably expressing TLR2 were transiently transfected with GyrB-fused wild-type MyD88 or mutant MyD88 with each cysteine residue replaced with a serine residue together with the NF-κB-driven luciferase gene and incubated for 16 h. At 6 h before the end of incubation, cells were treated with 200 μM SNAP. Cells were stimulated with 100 ng/ml Pam_3CSK_4 for 6 h, and then luciferase activity was measured. Each value is the mean ± SD ($n = 3$). (*, $P < 0.05$ for comparison with the wild-type group).

and residual proteins were observed even at 45 min after stimulation when cells were pretreated with SNAP (Fig. 2B). The effect of NO was not altered in the presence of the guanylate cyclase inhibitor ODQ or the cyclic-GMP-dependent protein kinase inhibitor KT5823 (data not shown). Notably, LPS-induced degradation of IRAK-1 and IκBα in HAECs was prevented by the irreversible thiol modification by *N*-ethylmaleimide (Fig. 2C), implying that the effect of NO on the signaling events depends on modification of cysteine residues.

To test whether NO alters the MyD88-dependent signal events, we utilized the MyD88-GyrB construct. Under coumermycin treatment of cells stably expressing MyD88-GyrB, MyD88-GyrB undergoes dimerization and mimics TLR-triggered typical MyD88-dependent functions, such as the activation of MAPKs and IKKs and secretion of proinflammatory cytokines (11). We found that coumermycin-dependent induction of NF-κB activation in HEK293 cells was suppressed by pretreatment with cells with NO donors (Fig. 3A). Coumermycin could induce phosphorylation of IκBα at Ser32 and Ser36, the target residues of IKKβ involved in degradation of IκBα (51), but SNAP pretreatment could suppress induction of the response (Fig. 3B). SNAP also suppressed coumermycin-induced phos-

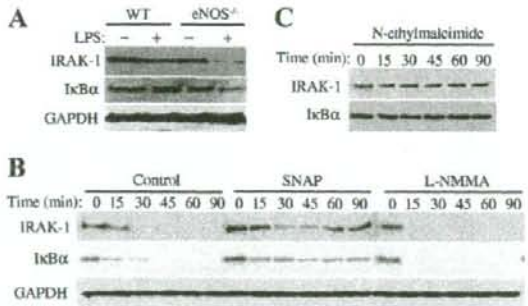

FIG. 2. NO suppresses LPS-induced degradation of IRAK-1 and IκBα. (A) Anesthetized wild-type (WT) and eNOS$^{-/-}$ mice intratracheally received *E. coli* LPS and mechanical ventilation. After 30 min of administration, lung was excised and then lysed for immunoblotting with anti-IRAK-1, anti-IκBα, and anti-GAPDH antibodies. (B) HAECs pretreated with 1 mM L-NMMA for 12 h or 0.25 mM SNAP for 1 h were stimulated with 10 ng/ml *E. coli* LPS for the indicated periods. The expression levels of IRAK-1 and IκBα were determined by immunoblot analysis. (C) HAECs pretreated with 0.1 mM *N*-ethylmaleimide for 10 min were stimulated with 10 ng/ml *E. coli* LPS for the indicated periods. The expression levels of IRAK-1 and IκBα were determined by immunoblot analysis.

phorylation of MAPKs (data not shown). The coumermycin-dependent dimerization of MyD88-GyrB induced interaction with TRAF6, consistent with a previous study (10), and we found that this interaction was reduced by SNAP treatment (Fig. 3C).

We found that NO and alteration of Cys113 and Cys216 residues of MyD88 did not alter the interaction of overexpressed MyD88 with IRAK-1 in HEK293 cells (Fig. 3D). However, NO clearly attenuated TLR4 stimulus (LPS)-dependent induction of MyD88–IRAK-1 interaction (Fig. 3E), suggesting that NO targets upstream signaling events of IRAK-1. It has been known that the recruitment of MyD88 to TLR2 or TLR4 is mediated by binding of the sorting adaptor TIRAP to the membrane phosphatidylinositol 4,5-bisphosphate, followed by interaction of MyD88 with TIRAP through TIR-TIR interaction (23). We examined whether NO affects the interaction of MyD88 with TIRAP. Overexpressed MyD88 interacted with TIRAP in HEK 293 cells (Fig. 3F). We found that treatment of the cells with the NO donor GSNO attenuated the interaction (Fig. 3F). We further investigated whether S nitrosylation of residues 113 and 216 is involved in MyD88-TIRAP interaction. Alteration of Cys residues did not affect the interaction (Fig. 3G). However, SNAP-induced attenuation of the interaction was reduced in the Cys216 mutant (Fig. 3G).

In HAECs, MyD88 was enriched with filamentous cytoskeletal structures and partly colocalized with β-actin (Fig. 4A). Additionally, a large part of MyD88 stably expressed in HEK293 cells was found in the cytoskeletal fraction (Fig. 4B). These findings are consistent with results of a previous study showing that MyD88 associates with β-actin in HeLa cells (22). Cytoskeletal MyD88 was separated from IRAK-1, which was found only in the cytoplasm (Fig. 4B), suggesting that MyD88 is maintained as an inactive state in cytoskeleton. We found that SNAP treatment altered such cytoskeletal localization of MyD88 into the cytoplasm (Fig. 4C). We further investigated the subcellular localization of MyD88 after TLR4 stimulation in 293-TLR4/MD2-CD14 cells stably expressing Flag-MyD88-GyrB. After LPS treatment, a part of MyD88 was transported to the cytoplasmic membrane from the cytoskeleton (Fig. 4D). However, SNAP treatment retarded such LPS-induced transportation of MyD88 (Fig. 4D). Although native PAGE analysis revealed that MyD88 formed a protein complex (more than 480 kDa) in HEK293 cells, SNAP treatment resulted in reduction in the size of the complex to approximately 450 kDa or 250 kDa, accompanied by an increase in concentration (Fig. 4E). Moreover, higher concentrations of SNAP further altered the complex to render a monomer (approximately 35 kDa) (Fig. 4E), implying disruption of functional MyD88 protein complex by NO.

Thus, NO has a capability to obstruct the MyD88 signing pathway through disruption of the multiple steps of protein interactions.

NO reversibly suppresses the MyD88 signaling events. S-nitrosylated proteins are known to undergo denitrosylation, by which regulatory effects of NO are conferred to control protein functions. We therefore investigated how S nitrosylation and denitrosylation affect MyD88-mediated signaling events. For this purpose, we utilized GSH because GSH had a capability to denitrosylate MyD88 (Fig. 1C). We found that GSH restored NO-induced impaired interaction of MyD88 with TIRAP (Fig. 4F). Furthermore, the NO-induced cytoplasmic localization of cytoskeletal MyD88 was restored by treatment of the cells with GSH (Fig. 4G). Thus, these results suggest that S nitrosylation alters the MyD88 pathway, and antioxidants or oxidoreductases restore such NO-derived actions, probably through denitrosylation.

NO reversibly suppresses TLR-mediated cellular responses. HAECs responded to multiple bacterial TLR agonistic molecules, Pam_3CSK_4 (for TLR1/TLR2), MALP-2 (for TLR2/TLR6), LPS (for TLR4), flagellin (for TLR5), and IL-1β, all of which are known to activate MyD88-dependnet signaling to induce production of the NF-κB-driven chemokine IL-8 after stimulation for 3 h (Fig. 5A). Predepletion of endogenous NO by L-NMMA resulted in a significant increase in IL-8 production induced by each stimulator (Fig. 5A), indicating that endogenous NO has a suppressive effect on the TLR-mediated cellular response. Furthermore, IL-8 production by each stimulator was suppressed in the presence of SNAP (Fig. 5A). The effect of NO donors was not altered in the presence of ODQ or KT5823 (data not shown). We investigated whether such a suppressive effect of NO can be restored because S nitrosylation is a reversible protein modification. However, it is difficult to examine the effects of antioxidants or oxidoreductases because the TLR signaling pathway is greatly affected by reactive oxygen species generated from NADPH oxidases (27, 34, 48). Indeed, treatment of cells with ascorbic acid, GSH, NAC, or the NADPH oxidase inhibitor DPI greatly impaired LPS-induced IL-8 production in HAECs (Fig. 5B). We therefore attempted to address whether the effect of NO is transient or persistent. For this purpose, HAECs were pretreated with SNAP for 1 h and washed two times to remove the NO donor. Then, at various times afterwards, the cells were stimulated with LPS and IL-8 production was measured. NO suppression of IL-8 production was gradually neutralized or restored in a

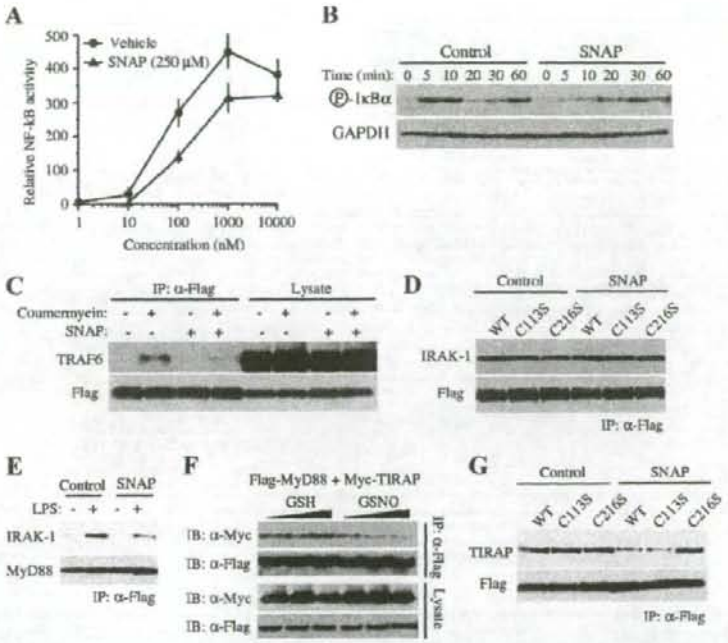

FIG. 3. Effects of NO on TLR-mediated signaling events. (A) HEK293 cells stably expressing MyD88-GyrB were transiently transfected with an NF-κB-driven luciferase gene and incubated for 24 h. Cells were pretreated with or without 0.25 mM SNAP for 1 h and then treated with 1 μM coumermycin for 3 h. Then, luciferase activity was measured. Each value is the mean ± SD (n = 3). (B) HEK293 cells stably expressing MyD88-GyrB were pretreated with or without 0.25 mM SNAP for 1 h and then treated with 1 μM coumermycin for the indicated periods. The phosphorylation of IκBα at Ser32/Ser36 was detected by immunoblot analysis. (C) HEK293 cells stably expressing MyD88-GyrB were pretreated with or without 0.25 mM SNAP for 1 h and then treated with 1 μM coumermycin for 20 min. Then, cell lysates were immunoprecipitated (IP) with anti-Flag antibody, followed by immunoblotting with anti-Flag and anti-TRAF6 antibodies. (D) HEK293 cells transiently expressing Flag-tagged wild-type (WT) or Cys residue (113 or 216) replacement MyD88 together with IRAK-1 were treated with 500 μM SNAP for 1 h. Then, cell lysates were immunoprecipitated with anti-Flag antibody, followed by immunoblotting with anti-Flag and anti-IRAK-1 antibodies. (E) 293-TLR4/MD2-CD14 cells stably expressing Flag-MyD88-GyrB were treated with or without 500 μM SNAP for 1 h and then stimulated with 100 ng/ml LPS for 20 min. Then, cell lysates were immunoprecipitated with anti-Flag antibody, followed by immunoblotting with anti-IRAK-1 and anti-Flag antibodies. (F) HEK293 cells transiently expressing Flag-tagged MyD88 together with Myc-tagged TIRAP were treated with GSH or GSNO (0, 100, and 500 μM) for 1 h. Then, cell lysates were immunoprecipitated with anti-Flag antibody, followed by immunoblotting (IB) with anti-Flag and anti-Myc antibodies. (G) HEK293 cells transiently expressing Flag-tagged wild-type or Cys residue (113 or 216) replacement MyD88 together with Myc-tagged TIRAP were treated with 500 μM SNAP for 1 h. Then, cell lysates were immunoprecipitated with anti-Flag antibody, followed by immunoblotting with anti-Flag and anti-IRAK-1 antibodies.

time-dependent manner, although the restrictive effect continues for several hours (Fig. 5C).

NO suppresses acute-phase immune responses to LPS in vivo. To explore how NO regulation of MyD88-dependent signaling reflects innate immune or proinflammatory responses in vivo, we utilized a popular animal model of sepsis induced by i.p. administration of LPS. We first investigated the cytokine responses as the major hallmark of innate immune responses. MIP-2 is known as one of the early LPS-responsive genes, the mRNA expression of which indeed showed a rapid rise and reached a peak within 1 h after LPS stimulation in mouse peritoneal macrophages (Fig. 6A). In contrast, IL-6 is known as a late LPS-responsive gene, the expression of which showed a gradual rise and reached a peak more than 4 h after stimulation (Fig. 6A). We determined the amounts of MIP-2 and IL-6 produced in the abdominal cavity 2 h after LPS administration in wild-type, $eNOS^{-/-}$, and $iNOS^{-/-}$ mice. Interestingly, $eNOS^{-/-}$ mice exhibited the most intensive production of MIP-2 (Fig. 6B). On the other hand, the most prominent production of IL-6 was observed in $iNOS^{-/-}$ mice (Fig. 6C). In contrast to these results, there was no significant difference in the amounts of MIP-2 and IL-6 production when the fluids were collected 12 h after LPS administration (data not shown). Thus, eNOS and iNOS at least exert a suppressive effect on early cytokine responses in vivo.

We further examined LPS-induced febrile response as a hallmark of acute-phase responses of inflammation. LPS is known to act as a pyrogen to induce TLR4-dependnet polyphasic fever (44). The major initiator of LPS fever is generated prostaglandin E2, which stimulates thermoregulatory neurons and elevates body core temperature (3). LPS can directly induce prostaglandin E2 generation through the MyD88-dependent signaling pathway (47). The first-phase febrile response in $eNOS^{-/-}$ mice occurred significantly earlier than that in wild-

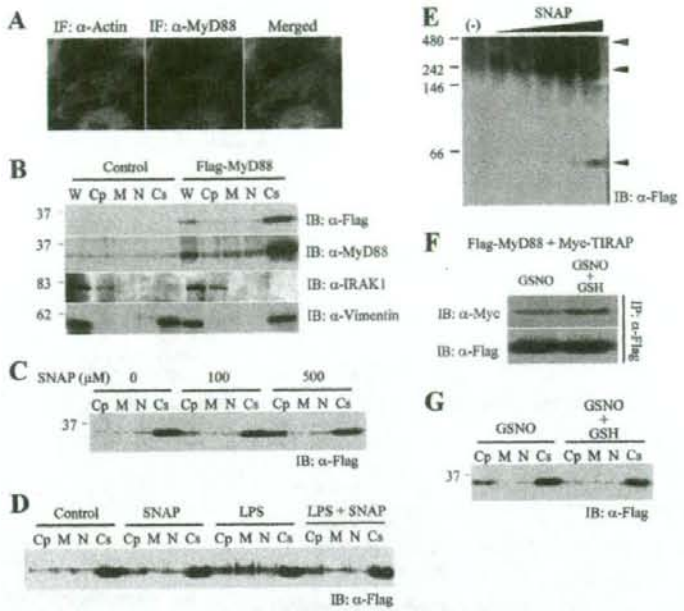

FIG. 4. Reverse of the suppressive effect of NO by GSH. (A) HAECs were fixed and stained immunofluorescently (IF) with anti-β-actin antibody (green, left), anti-MyD88 antibody (red, middle), and Hoechst33342 (blue, right). (B) Parental HEK293 cells and HEK293 cells stably expressing Flag-MyD88 were fractionated into the cytoplasm (Cp), cytoplasmic membrane (M), nucleus (N), and cytoskeleton (Cs). Whole-cell lysates (W) were also obtained. The fractions were assessed by immunoblotting (IB) with anti-Flag, anti-MyD88, anti-IRAK-1, and anti-vimentin antibodies. (C) HEK293 cells stably expressing Flag-MyD88 were treated with the indicated concentration of SNAP for 1 h and fractionated into each fraction. The fractions were assessed by immunoblotting with anti-Flag antibody. (D) 293-TLR4/MD2-CD14 cells stably expressing Flag-MyD88-GyrB were treated with or without 500μM SNAP for 1 h and then stimulated with 100 ng/ml LPS for 20 min. Cells were then fractionated into each fraction. The fractions were assessed by immunoblotting with anti-Flag antibody. (E) HEK293 cells stably expressing Flag-MyD88 were treated with or without SNAP (10, 50, 125, 250, and 500 μM) for 1 h. Then, cell lysates were assessed by blue native PAGE and immunoblotting with anti-Flag antibody. (F) HEK293 cells transiently expressing Flag-MyD88 and Myc-tagged TIRAP were treated with 500 μM GSNO for 1 h and then with or without 500 μM GSH for 15 min. Then, cell lysates were immunoprecipitated with anti-Flag antibody, followed by immunoblotting with anti-Flag and anti-Myc antibodies. (G) HEK293 cells stably expressing Flag-MyD88 were treated with the 500 μM GSNO for 1 h and then with or without 500 μM GSH for 15 min. The cells were fractionated into each fraction, followed by immunoblotting with anti-Flag antibody.

type or iNOS$^{-/-}$ mice (Fig. 6D), indicating that NO from eNOS suppresses the initiation of the response. However, eNOS deficiency did not alter the magnitude of febrile response compared with that for wild-type mice, suggesting that the suppressive effect of NO is not persistent. On the other hand, a transient decrease in fever was found in wild-type and eNOS$^{-/-}$ mice at about 70 min after LPS administration but not in iNOS$^{-/-}$ mice (Fig. 6D), indicating that NO from iNOS suppresses promotion of the response. Thus, these results suggest that NO generated from eNOS and iNOS exerts a suppressive effect on acute-phase inflammatory responses to LPS in vivo, probably through S nitrosylation.

DISCUSSION

Our findings imply that MyD88-dependent signaling events are affected by S nitrosylation, by which innate immune signal transduction might be reduced in living organisms. The effect of NO is transient and is restored by antioxidants or oxidoreductases, in which protein denitrosylation plays an important role. Although the physiological significance of such regulation of TLR signal transduction is unsettled, NO is likely to retard signaling cascades through S nitrosylation, by which rapid and precipitous signaling reactions may be initially or inductively relieved. Such an effect may reflect an adequate regulation of acute-phase inflammatory responses, leading to limitation of the degree of inflammation and resolution of inflammation.

We found that the suppressive effect of NO on TLR-mediated cellular responses was transient and degraded in a time-dependent manner (Fig. 5C). The specificity of NO regulation may be conferred by the spatial regulation of S nitrosylation within or between proteins and the stimulus-coupled temporal regulation through denitrosylation (14). Signal transduction by ligand-receptor interactions is thought to trigger denitrosylation, restoring substantial protein functions. For example, reduction of the functions of caspase-3 and IKKβ by S nitrosylation is restored by FasL-Fas interaction and TNF-α–TNFR interaction, respectively (30, 39). Thus, it is possible that TLR ligation-dependent protein denitrosylation also facilitates the restoration of NO suppression although the mechanism of denitrosylation has been poorly studied. Protein denitrosyla-

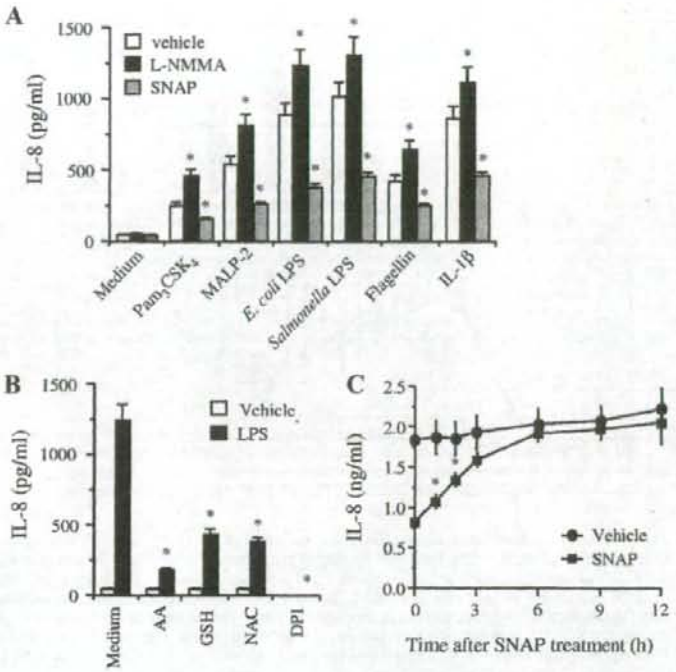

FIG. 5. NO reversibly suppresses TLR-mediated cellular responses. (A) HAECs pretreated with 1 mM L-NMMA for 12 h or 0.25 mM SNAP for 1 h were stimulated with 1 μg/ml Pam_3CSK_4, 100 nM MALP-2, 10 ng/ml *E. coli* LPS, 10 ng/ml *Salmonella* LPS, 5 μg/ml flagellin, and 10 ng/ml IL-1β for 3 h. Then, production of IL-8 was determined by ELISA. Each value is the mean ± SD ($n = 3$). *, $P < 0.01$ for comparison with the vehicle group. (B) HAECs were stimulated with 10 ng/ml *E. coli* LPS for 3 h in the presence or absence of 1 mM ascorbic acid (AA), 1 mM GSH, 1 mM NAC, or 20 μM DPI. Then production of IL-8 was determined by ELISA. Each value is the mean ± SD ($n = 3$). (*, $P < 0.01$ for comparison with the vehicle group). (C) HAECs were treated with 0.25 mM SNAP for 1 h and then at various times afterwards stimulated with 10 ng/ml *E. coli* LPS for 3 h. Then, production of IL-8 was determined by ELISA. Each value is the mean ± SD ($n = 3$). (*, $P < 0.01$ for comparison with the vehicle group).

tion is catalyzed by antioxidants or oxidoreductases, including ascorbic acid, thioredoxin-thioredoxin reductase, superoxide dismutase GSH, and GSNO reductase (14, 15, 50, 53). S-nitrosylated MyD88 can be denitrosylated in the presence of ascorbic acid and GSH in vitro (Fig. 1C). Although it is still unclear how TLR ligation activates cellular redox activity, LPS has a potential to activate cellular redox activity and transition of GSH into GSNO (41). More details of TLR-mediated protein S nitrosylation and denitrosylation should be investigated in future studies.

TLR ligation can initiate recruitment of MyD88 to the receptor complex through TIR-TIR interaction. In the case of TLR2 and TLR4, the sorting adaptor TIRAP is essentially required to recruit MyD88 (23). MyD88 then dissociates from the receptor complex and recruits IRAK-1 (and IRAK-4) through death domain (DD)-DD interaction, inducing TRAF6-mediated signaling events and ubiquitin ligation to IRAK-1 or IκBα, followed by proteasomal degradation (1). Nevertheless, how MyD88 can be initially controlled to be recruited to TLRs has remained unclear. We found that a large part of cellular MyD88 existed in the cytoskeleton and associated with β-actin (Fig. 4A and B), wherein MyD88 formed a complex dissociated from IRAK-1 (Fig. 4B). Our finding suggests that MyD88 preferentially interacts with the cytoskeleton as an inactive form, followed by release into the cytoplasm and recruitment to TLRs after ligation-dependent actin rearrangement. Indeed, inhibition of actin rearrangement by cytochalasin D suppresses LPS-induced signal transduction and cytokine production (5). In addition, cytochalasin D also alters TIRAP recruitment to the cytoplasmic membrane (23). NO restriction of MyD88 function may be achieved through disruption of the protein complex and dissociation of MyD88 from the actin cytoskeleton to the cytoplasm (Fig. 4A to E). NO also reduces the interaction of MyD88 with TIRAP (Fig. 3). These effects may ultimately result in mitigated potential for the ligation-dependent recruitment of MyD88 to TLRs.

We found that S nitrosylation of MyD88 plays some roles in NO modulation of TLR signal transduction. Interestingly, eight of the nine cysteine residues of MyD88 are concentrated in the TIR domain, but the C-terminal DD contains no cysteine residue, suggesting that cysteine modification affects TIR-TIR interaction but not DD-DD interaction. Indeed, NO attenuated the interaction of MyD88 with TIRAP but not that with IRAK-1 (Fig. 3). This result is supported by the result found by Xiong et al. (52) showing that SNAP treatment did

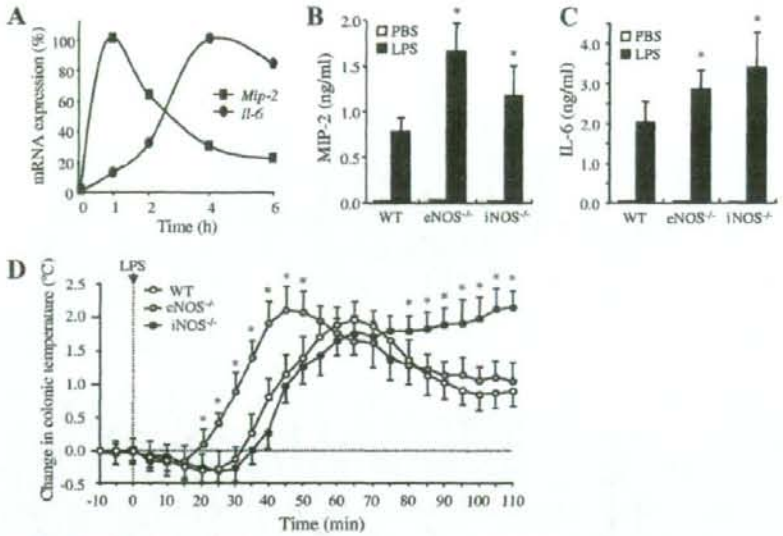

FIG. 6. Roles of eNOS and iNOS in early innate immune responses in vivo. (A) Peritoneal macrophages from wild-type mice were stimulated with 100 ng/ml LPS and 10 ng/ml gamma interferon for the indicated periods. Then, expression levels of mRNAs of *Mip-2* and *Il-6* were determined by quantitative PCR. Percent mRNA expression was calculated by taking the maximum values of mRNA levels of *Mip-2* and *Il-6* as 100%. (B, C) Wild-type (WT), eNOS$^{-/-}$, and iNOS$^{-/-}$ mice were i.p. treated with LPS. After 2 h, PBS was injected into the abdominal cavity and fluids were collected for measurement of the amounts of MIP-2 (B) and IL-6 (C) by ELISA. Each value is the mean ± SD ($n = 6$). (*, $P < 0.01$ for comparison with wild-type mice). (D) Wild-type, eNOS$^{-/-}$, and iNOS$^{-/-}$ mice were i.p. treated with LPS. The colonic temperature was monitored at 5-min intervals during a period of 10 min before and 120 min after LPS administration. Each value is the mean ± SD ($n = 6$). (*, $P < 0.01$ for comparison with wild-type mice).

not affect the interaction of MyD88 with IRAK-1 in mouse macrophages. Although S nitrosylation of the Cys216 residue of MyD88 may participate in the NO regulation of TLR signal transduction, it is likely that this modification does not have a dominant effect, because Cys216 was not essential for activation of downstream signaling (Fig. 1G). NO modification of Cys216 may yield a slight structural change in the base of the TIR domain, resulting in slightly reduced interaction with a counterpart TIR domain of TIRAP. Alternatively, NO may antagonize other reversible modifications, such as palmitoylation or disulfide bonding to a counterpart molecule, leading to transient impairment of MyD88 functioning. Also, other unknown mechanisms for MyD88 regulation may be negatively influenced by S nitrosylation.

We found that eNOS and iNOS differentially regulate LPS-induced acute-phase immune responses in vivo (Fig. 6). Although the amount of NO derived from eNOS is comparatively small, NO is steadily generated from endothelial cells as a vasodilatory gas that continually maintains an antiproliferative and antiapoptotic environment in vasculatures (16). Simultaneously, eNOS increases the amounts of cellular S-nitrosylated proteins and circulating NO donors by nitrosylating GSH and albumin (40). Such functions of NO from eNOS may systemically reduce cellular reactivity to a TLR stimulus to maintain a weak tolerance, which may lead to prevention of a rapid rise of inflammation. In contrast, NO from iNOS is generated in large quantities and exerts a strong antimicrobial action, although NO from eNOS also has an antimicrobial property (4, 29). The large amount of NO derived from iNOS is thought to disrupt cellular signaling cascades, resulting in anti-inflammatory or immunosuppressive effects. Such functions of NO from iNOS may regionally reduce cellular reactivity to TLR recognition of pathogens to initiate an inducible tolerance, which may transiently prevent promotion of excess inflammatory responses, although excess NO production ultimately results in nitrosative stress and apoptotic cell death (12, 26).

Our study proposes that TLR signal transduction involves an oxidative protein modification by NO and its redox regulation. NO may exert other effects, such as activation of cyclic-GMP-dependent signaling, on TLR signaling events, but such effects may not be dominant, at least in the acute-phase innate immune responses. Further investigations will be necessary to clarify more details about the relationship between such NO regulation and physiological or pathophysiological innate immune responses.

ACKNOWLEDGMENTS

We thank Margaret K. Offermann (Emory University School of Medicine) for providing DNA constructs of human MyD88 and TIRAP.

This work was supported by grants-in-aid for Scientific Research on Priority Areas (19041079 to T. Into) and for Young Scientists (B: 18791363 to T. Into), provided by the Ministry of Education, Culture, Sports, Science and Technology, Japan.

REFERENCES

1. **Akira, S., and K. Takeda.** 2004. Toll-like receptor signalling. Nat. Rev. Immunol. 4:499–511.

2. **Akira, S., S. Uematsu, and O. Takeuchi.** 2006. Pathogen recognition and innate immunity. Cell **124**:783–801.
3. **Blatteis, C. M., E. Sehic, and S. Li.** 2000. Pyrogen sensing and signaling: old views and new concepts. Clin. Infect. Dis. **31**:S168–177.
4. **Bogdan, C.** 2001. Nitric oxide and the immune response. Nat. Immunol. **2**:907–916.
5. **Dai, Q., and S. B. Pruett.** 2006. Ethanol suppresses LPS-induced Toll-like receptor 4 clustering, reorganization of the actin cytoskeleton, and associated TNF-α production. Alcohol Clin. Exp. Res. **30**:1436–1444.
6. **Dimmeler, S., J. Haendeler, M. Nehls, and A. M. Zeiher.** 1997. Suppression of apoptosis by nitric oxide via inhibition of interleukin-1β-converting enzyme (ICE)-like and cysteine protease protein (CPP)-32-like proteases. J. Exp. Med. **185**:601–607.
7. **Farrar, M. A., I. Alberol, and R. M. Perlmutter.** 1996. Activation of the Raf-1 kinase cascade by coumermycin-induced dimerization. Nature **383**:178–181.
8. **Forrester, M. T., M. W. Foster, and J. S. Stamler.** 2007. Assessment and application of the biotin switch technique for examining protein *S*-nitrosylation under conditions of pharmacologically induced oxidative stress. J. Biol. Chem. **282**:13977–13983.
9. **Forstermann, U., J. P. Boissel, and H. Kleinert.** 1998. Expressional control of the 'constitutive' isoforms of nitric oxide synthase (NOS I and NOS III). FASEB J. **12**:773–790.
10. **Ghosh, S., and M. Karin.** 2002. Missing pieces in the NF-κB puzzle. Cell **109**:S81–96.
11. **Häcker, H., V. Redecke, B. Blagoev, I. Kratchmarova, L. C. Hsu, G. G. Wang, M. P. Kamps, E. Raz, H. Wagner, G. Hacker, M. Mann, and M. Karin.** 2006. Specificity in Toll-like receptor signalling through distinct effector functions of TRAF3 and TRAF6. Nature **439**:204–207.
12. **Hara, M. R., N. Agrawal, S. F. Kim, M. B. Cascio, M. Fujimuro, Y. Ozeki, M. Takahashi, J. H. Cheah, S. K. Tankou, L. D. Hester, C. D. Ferris, S. D. Hayward, S. H. Snyder, and A. Sawa.** 2005. *S*-nitrosylated GAPDH initiates apoptotic cell death by nuclear translocation following Siah1 binding. Nat. Cell Biol. **7**:665–674.
13. **Hayden, M. S., A. P. West, and S. Ghosh.** 2006. NF-κB and the immune response. Oncogene **25**:6758–6780.
14. **Hess, D. T., A. Matsumoto, S. O. Kim, H. E. Marshall, and J. S. Stamler.** 2005. Protein *S*-nitrosylation: purview and parameters. Nat. Rev. Mol. Cell Biol. **6**:150–166.
15. **Hoffmann, J., J. Haendeler, A. M. Zeiher, and S. Dimmeler.** 2001. TNFα and oxLDL reduce protein *S*-nitrosylation in endothelial cells. J. Biol. Chem. **276**:41383–41387.
16. **Ignarro, L. J.** 2002. Nitric oxide as a unique signaling molecule in the vascular system: a historical overview. J. Physiol. Pharmacol. **53**:503–514.
17. **Into, T., J. Dohkan, M. Inomata, M. Nakashima, K. Shibata, and K. Matsushita.** 2007. Synthesis and characterization of a dipalmitoylated lipopeptide derived from paralogous lipoproteins of *Mycoplasma pneumoniae*. Infect. Immun. **75**:2253–2259.
18. **Into, T., Y. Kanno, J. Dohkan, M. Nakashima, M. Inomata, K. Shibata, C. J. Lowenstein, and K. Matsushita.** 2007. Pathogen recognition by Toll-like receptor 2 activates Weibel-Palade body exocytosis in human aortic endothelial cells. J. Biol. Chem. **282**:8134–8141.
19. **Into, T., and K. Shibata.** 2005. Apoptosis signal-regulating kinase 1-mediated sustained p38 mitogen-activated protein kinase activation regulates mycoplasmal lipoprotein- and staphylococcal peptidoglycan-triggered Toll-like receptor 2 signalling pathways. Cell. Microbiol. **7**:1305–1317.
20. **Iwasaki, A., and R. Medzhitov.** 2004. Toll-like receptor control of the adaptive immune responses. Nat. Immunol. **5**:987–995.
21. **Jaffrey, S. R., H. Erdjument-Bromage, C. D. Ferris, P. Tempst, and S. H. Snyder.** 2001. Protein *S*-nitrosylation: a physiological signal for neuronal nitric oxide. Nat. Cell Biol. **3**:193–197.
22. **Jaunin, F., K. Burns, J. Tschopp, T. E. Martin, and S. Fakan.** 1998. Ultrastructural distribution of the death-domain-containing MyD88 protein in HeLa cells. Exp. Cell Res. **243**:67–75.
23. **Kagan, J. C., and R. Medzhitov.** 2006. Phosphoinositide-mediated adaptor recruitment controls Toll-like receptor signaling. Cell **125**:943–955.
24. **Karin, M., and F. R. Greten.** 2005. NF-κB: linking inflammation and immunity to cancer development and progression. Nat. Rev. Immunol. **5**:749–759.
25. **Kelleher, Z. T., A. Matsumoto, J. S. Stamler, and H. E. Marshall.** 2007. NOS2 regulation of NF-κB by *S*-nitrosylation of p65. J. Biol. Chem. **282**:30667–30672.
26. **Kim, K. M., P. K. Kim, Y. G. Kwon, S. K. Bai, W. D. Nam, and Y. M. Kim.** 2002. Regulation of apoptosis by nitrosative stress. J. Biochem. Mol. Biol. **35**:127–133.
27. **Laroux, F. S., X. Romero, L. Wetzler, P. Engel, and C. Terhorst.** 2005. MyD88 controls phagocyte NADPH oxidase function and killing of gram-negative bacteria. J. Immunol. **175**:5596–5600.
28. **Lawrence, T., M. Bebien, G. Y. Liu, V. Nizet, and M. Karin.** 2005. IKKα limits macrophage NF-κB activation and contributes to the resolution of inflammation. Nature **434**:1138–1143.
29. **MacMicking, J., Q. W. Xie, and C. Nathan.** 1997. Nitric oxide and macrophage function. Annu. Rev. Immunol. **15**:323–350.
30. **Mannick, J. B., A. Hausladen, L. Liu, D. T. Hess, M. Zeng, Q. X. Miao, L. S. Kane, A. J. Gow, and J. S. Stamler.** 1999. Fas-induced caspase denitrosylation. Science **284**:651–654.
31. **Mannick, J. B., C. Schonhoff, N. Papeta, P. Ghafourifar, M. Szibor, K. Fang, and B. Gaston.** 2001. *S*-Nitrosylation of mitochondrial caspases. J. Cell Biol. **154**:1111–1116.
32. **Marshall, H. E., D. T. Hess, and J. S. Stamler.** 2004. *S*-nitrosylation: physiological regulation of NF-κB. Proc. Natl. Acad. Sci. USA **101**:8841–8842.
33. **Marshall, H. E., and J. S. Stamler.** 2001. Inhibition of NF-κB by *S*-nitrosylation. Biochemistry **40**:1688–1693.
34. **Matsuzawa, A., K. Saegusa, T. Noguchi, C. Sadamitsu, H. Nishitoh, S. Nagai, S. Koyasu, K. Matsumoto, K. Takeda, and H. Ichijo.** 2005. ROS-dependent activation of the TRAF6-ASK1-p38 pathway is selectively required for TLR4-mediated innate immunity. Nat. Immunol. **6**:587–592.
35. **Medzhitov, R., P. Preston-Hurlburt, and C. A. Janeway, Jr.** 1997. A human homologue of the Drosophila Toll protein signals activation of adaptive immunity. Nature **388**:394–397.
36. **Medzhitov, R., P. Preston-Hurlburt, E. Kopp, A. Stadlen, C. Chen, S. Ghosh, and C. A. Janeway, Jr.** 1998. MyD88 is an adaptor protein in the hToll/IL-1 receptor family signaling pathways. Mol. Cell **2**:253–258.
37. **Miggin, S. M., E. Palsson-McDermott, A. Dunne, C. Jefferies, E. Pinteaux, K. Banahan, C. Murphy, P. Moynagh, M. Yamamoto, S. Akira, N. Rothwell, D. Golenbock, K. A. Fitzgerald, and L. A. O'Neill.** 2007. NF-κB activation by the Toll-IL-1 receptor domain protein MyD88 adapter-like is regulated by caspase-1. Proc. Natl. Acad. Sci. USA **104**:3372–3377.
38. **Park, H. S., J. W. Yu, J. H. Cho, M. S. Kim, S. H. Huh, K. Ryoo, and E. J. Choi.** 2004. Inhibition of apoptosis signal-regulating kinase 1 by nitric oxide through a thiol redox mechanism. J. Biol. Chem. **279**:7584–7590.
39. **Reynaert, N. L., K. Ckless, S. H. Korn, N. Vos, A. S. Guala, E. F. Wouters, A. van der Vliet, and Y. M. Janssen-Heininger.** 2004. Nitric oxide represses inhibitory κB kinase through *S*-nitrosylation. Proc. Natl. Acad. Sci. USA **101**:8945–8950.
40. **Richardson, G., and N. Benjamin.** 2002. Potential therapeutic uses for *S*-nitrosothiols. Clin. Sci. (London) **102**:99–105.
41. **Rubin, D. B., G. Reznik, E. A. Weiss, and P. R. Young.** 2000. Non-protein thiols flux to *S*-nitrosothiols in endothelial cells: an LPS redox signal. Shock **14**:200–207.
42. **Stamler, J. S., S. Lamas, and F. C. Fang.** 2001. Nitrosylation. The prototypic redox-based signaling mechanism. Cell **106**:675–683.
43. **Stamler, J. S., D. I. Simon, J. A. Osborne, M. E. Mullins, O. Jaraki, T. Michel, D. J. Singel, and J. Loscalzo.** 1992. *S*-nitrosylation of proteins with nitric oxide: synthesis and characterization of biologically active compounds. Proc. Natl. Acad. Sci. USA **89**:444–448.
44. **Steiner, A. A., S. Chakravarty, A. Y. Rudaya, M. Herkenham, and A. A. Romanovsky.** 2006. Bacterial lipopolysaccharide fever is initiated via Toll-like receptor 4 on hematopoietic cells. Blood **107**:4000–4002.
45. **Steiner, A. A., A. Y. Rudaya, A. I. Ivanov, and A. A. Romanovsky.** 2004. Febrigenic signaling to the brain does not involve nitric oxide. Br. J. Pharmacol. **141**:1204–1213.
46. **Thoma-Uszynski, S., S. Stenger, O. Takeuchi, M. T. Ochoa, M. Engele, P. A. Sieling, P. F. Barnes, M. Rollinghoff, P. L. Bolcskei, M. Wagner, S. Akira, M. V. Norgard, J. T. Belisle, P. J. Godowski, B. R. Bloom, and R. L. Modlin.** 2001. Induction of direct antimicrobial activity through mammalian Toll-like receptors. Science **291**:1544–1547.
47. **Uematsu, S., M. Matsumoto, K. Takeda, and S. Akira.** 2002. Lipopolysaccharide-dependent prostaglandin E(2) production is regulated by the glutathione-dependent prostaglandin E(2) synthase gene induced by the Toll-like receptor 4/MyD88/NF-IL6 pathway. J. Immunol. **168**:5811–5816.
48. **Vulcano, M., S. Dusi, D. Lissandrini, R. Badolato, P. Mazzi, E. Riboldi, E. Borroni, A. Calleri, M. Donini, A. Plebani, L. Notarangelo, T. Musso, and S. Sozzani.** 2004. Toll receptor-mediated regulation of NADPH oxidase in human dendritic cells. J. Immunol. **173**:5749–5756.
49. **Wang, W., A. Mitra, B. Poole, S. Faik, M. S. Lucia, S. Tayal, and R. Schrier.** 2004. Endothelial nitric oxide synthase-deficient mice exhibit increased susceptibility to endotoxin-induced acute renal failure. Am. J. Physiol. Renal Physiol. **287**:F1044–F1048.
50. **West, M. B., B. G. Hill, Y. T. Xuan, and A. Bhatnagar.** 2006. Protein glutathiolation by nitric oxide: an intracellular mechanism regulating redox protein modification. FASEB J. **20**:1715–1717.
51. **Woronicz, J. D., X. Gao, Z. Cao, M. Rothe, and D. V. Goeddel.** 1997. IκB kinase-β: NF-κB activation and complex formation with IκB kinase-α and NIK. Science **278**:866–869.
52. **Xiong, H., C. Zhu, F. Li, R. Hegazi, K. He, M. Babyatsky, A. J. Bauer, and S. E. Plevy.** 2004. Inhibition of interleukin-12 p40 transcription and NF-κB activation by nitric oxide in murine macrophages and dendritic cells. J. Biol. Chem. **279**:10776–10783.
53. **Yamawaki, H., J. Haendeler, and B. C. Berk.** 2003. Thioredoxin: a key regulator of cardiovascular homeostasis. Circ. Res. **93**:1029–1033.

THE JOURNAL OF BIOLOGICAL CHEMISTRY VOL. 282, NO. 11, pp. 8134–8141, March 16, 2007

Pathogen Recognition by Toll-like Receptor 2 Activates Weibel-Palade Body Exocytosis in Human Aortic Endothelial Cells*

Received for publication, October 24, 2006, and in revised form, December 22, 2006 Published, JBC Papers in Press, January 16, 2007, DOI 10.1074/jbc.M609962200

Takeshi Into[‡1], Yosuke Kanno[‡], Jun-ichi Dohkan[‡], Misako Nakashima[‡], Megumi Inomata[‡], Ken-ichiro Shibata[§], Charles J. Lowenstein[¶], and Kenji Matsushita[‡]

From the [‡]Department of Oral Disease Research, National Institute for Longevity Sciences, National Center for Geriatrics and Gerontology, 36-3 Gengo, Morioka, Obu, Aichi 474-8522, Japan, the [§]Laboratory of Oral Molecular Microbiology, Department of Oral Pathobiological Science, Hokkaido University Graduate School of Dental Medicine, Sapporo 060-8586, Japan, and the [¶]Departments of Medicine and Pathology, Johns Hopkins University School of Medicine, Baltimore, Maryland 21205

The endothelial cell-specific granule Weibel-Palade body releases vasoactive substances capable of modulating vascular inflammation. Although innate recognition of pathogens by Toll-like receptors (TLRs) is thought to play a crucial role in promotion of inflammatory responses, the molecular basis for early-phase responses of endothelial cells to bacterial pathogens has not fully been understood. We here report that human aortic endothelial cells respond to bacterial lipoteichoic acid (LTA) and synthetic bacterial lipopeptides, but not lipopolysaccharide or peptidoglycan, to induce Weibel-Palade body exocytosis, accompanied by release or externalization of the storage components von Willebrand factor and P-selectin. LTA could activate rapid Weibel-Palade body exocytosis through a TLR2- and MyD88-dependent mechanism without *de novo* protein synthesis. This process was at least mediated through MyD88-dependent phosphorylation and activation of phospholipase Cγ. Moreover, LTA activated interleukin-1 receptor-associated kinase-1-dependent delayed exocytosis with *de novo* protein synthesis and phospholipase Cγ-dependent activation of the NF-κB pathway. Increased TLR2 expression by transfection or interferon-γ treatment increased TLR2-mediated Weibel-Palade body exocytosis, whereas reduced TLR2 expression under laminar flow decreased the response. Thus, we propose a novel role for TLR2 in induction of a primary proinflammatory event in aortic endothelial cells through Weibel-Palade body exocytosis, which may be an important step for linking innate recognition of bacterial pathogens to vascular inflammation.

The onset of inflammatory responses of vascular endothelial cells plays crucial roles in recruitment of immune cells, thrombus formation, and development of vascular inflammation or atherosclerosis. Early endothelial activation involves dual phases: rapid translocation of P-selectin to the endothelial surface and slower synthesis and expression of adhesion molecules such as ICAM-1 (intercellular adhesion molecule 1).[2] The former process is accompanied by rapid exocytosis of Weibel-Palade bodies, which are endothelial cell-specific storage granules that contain vascular modulators, including von Willebrand factor (VWF), P-selectin, IL-8, eotaxin-3, endothelin-1, CD63/lamp3, osteoprotegerin, and angiopoietin-2 (1, 2). During Weibel-Palade body exocytosis, these proteins are transported to the outside of the cell upon stimulation or vascular damage and may control local or systemic pathobiological effects, including thrombosis and atherogenesis. Regulated Weibel-Palade body exocytosis is known to be initiated through an increase of intracellular calcium level after stimulation with various secretagogues, including calcium ionophores, thrombin, histamine, TNF-α, and extracellular ATP (1, 2).

Recently, excess innate immune responses of vessel walls or endothelium to invading pathogens have been suggested to be linked to atherogenesis. Several common bacterial infectious agents or invasive pathogens, such as *Chlamydia pneumoniae*, *Helicobacter pylori*, *Porphyromonas gingivalis*, and oral commensal bacteria, have so far been detected in vessel walls or atherosclerotic lesions in humans (3, 4). However, the linkage between artery endothelial innate recognition of such pathogens and inflammatory responses has not been fully elucidated.

For the detection of invasive bacteria in host defense, several Toll-like receptors (TLRs) are employed to identify molecular motifs that usually compose bacterial bodies (5). Among TLR members in humans, TLR2 detects the widest range of common bacterial constituents, such as lipoteichoic acids (LTA),

* This work was supported by a Grant-in-aid for Young Scientists ((B):18791363 to T. I.) provided by the Ministry of Education, Culture, Sports, Science and Technology and by Mitsui, Life Social Welfare Foundation, Aich Cancer Research Foundation, Mitsubishi Pharma Research Foundation, Mochida Memorial Foundation for Medical and Pharmaceutical Research, and Suzuken Memorial Foundation (to K. M.). The costs of publication of this article were defrayed in part by the payment of page charges. This article must therefore be hereby marked "*advertisement*" in accordance with 18 U.S.C. Section 1734 solely to indicate this fact.

[1] To whom correspondence should be addressed. Tel.: 81-562-44-5651; Fax: 81-562-46-8684; E-mail: into@nils.go.jp.

[2] The abbreviations used are: ICAM-1, intercellular adhesion molecule 1; BAPTA-AM, 1,2-bis(2-aminophenoxy)ethane-*N,N,N',N'*-tetraacetic acid-acetoxymethyl ester; FSL-1, synthetic *S*-dipalmitoylglyceryl-CGDPKHPKSF derived from *Mycoplasma salivarium*; HAEC, human aortic endothelial cell; HUVEC, human umbilical vein endothelial cell; IRAK, IL-1R-associated kinase; LTA, lipoteichoic acid; MALP-2, synthetic *S*-dipalmitoylglyceryl-CGNNDESNISFKEK derived from *Mycoplasma fermentans*; Pam_3CSK_4, synthetic *N*-palmitoyl-*S*-dipalmitoylglyceryl-CSKKKK derived from *E. coli*; PGN, peptidoglycan; PLC, phospholipase C; TLR, Toll-like receptor; TNF, tumor necrosis factor; TNFR, TNF receptor; TRAF, TNFR-associated factor; VWF, von Willebrand factor; LPS, lipopolysaccharide; IL-1R, interleukin-1 receptor; siRNA, small interference RNA; ELISA, enzyme-linked immunosorbent assay; PI3K, phosphatidylinositol 3-kinase; IFN, interferon.

peptidoglycans (PGN), bacterial di- or triacylated lipoproteins or lipopeptides, lipoarabinomannans, porins, and fimbriae (5–8). TLR4 and TLR5 contribute to the recognition of only a few bacterial components, *i.e.* LPS and flagellin (9, 10). Because TLR1 and TLR6 participate in the accurate discrimination of molecular structures by TLR2 as coreceptors, several molecules, including CD14, CD36, and LOX-1, further facilitate the interactions of TLR2 with bacterial pathogens (5, 11, 12). After recognition of cognate agonists, endothelial TLRs activate the classic Toll/IL-1R signaling pathway utilizing MyD88 and IL-1R-associated kinase (IRAK)-1, which ultimately activate a TNFR-associated factor (TRAF) 6 complex and IκBs and the release and translocation of active NF-κB to the nucleus. The artery endothelial NF-κB signaling pathways downstream of TLRs are thought to participate in the development of artery inflammatory diseases or atherogenesis through the promotion of the expression of a large number of proinflammatory mediators and adhesion molecules (13–15). However, it is still not known whether artery endothelial TLRs are primary initiators or modulators of the diseases.

In this study, we investigated the early-phase proinflammatory responses of human aortic endothelial cells (HAECs) to bacterial cell wall constituents. We found that recognition of bacterial constituents by TLRs, especially by TLR2 but not TLR4, could activate Weibel-Palade body exocytosis. We further investigated the involvement of MyD88 in regulation of the cell response.

EXPERIMENTAL PROCEDURES

Reagents, Chemicals, and Antibodies—LTA and PGN from *Staphylococcus aureus* and LPS from *Escherichia coli* O26:B6 were obtained from Sigma-Aldrich. Rough-form LPS from *Salmonella minnesota* R595 and flagellin from *Salmonella typhimurium* strain 14028 were obtained from Alexis Biochemicals. Pam_3CSK_4 (16) was obtained from InvivoGen. Preparation of FSL-1 and MALP-2 was described previously (17–19). A23187, the cell-permeable calcium chelator 1,2-bis(2-aminophenoxy)ethane-*N*,*N*,*N*′,*N*′-tetraacetic acid-acetoxymethyl ester (BAPTA-AM), cycloheximide, and the phospholipase C (PLC) γ inhibitor U-73122 were purchased from Sigma. LY294002 was purchased from Calbiochem. Monoclonal antibodies to human TLR2, TL2.1 (BD Biosciences), TL2.3 (eBioscience), and IMG-319 (Immugenex), were purchased for a TLR2 blocking study and flow cytometry. Antibodies to PLCγ1 and phosphorylated PLCγ1 (Y783) were obtained from Cell Signaling Biotechnology. All other reagents were obtained from Sigma-Aldrich unless otherwise indicated.

DNA Cloning—A human TLR2-encoding plasmid was prepared as described previously (17). The dominant negative TLR2 (P681H) was constructed using a QuikChange II site-directed mutagenesis kit (Stratagene) according to the manufacturer's instructions.

Cell Culture and Transfection of siRNA—HEK293 cells and human monocytic THP-1 cells were grown as described previously (20). HAECs and HUVECs were grown in endothelial growth medium-2 (Camblex) as described previously (21). These endothelial cells were used for experiments from passages 4 to 8. All of the gene-specific siRNA oligonucleotides for human TLR1, TLR2, TLR6, MyD88, and IRAK-1 and a control oligonucleotide were purchased from Dharmacon. Although the sequences were not provided by the manufacturer, significant suppressive effects on the respective gene expression could be confirmed by reverse transcription-PCR compared with the control transfection (data not shown). For the transfection of siRNA, confluent HAECs or HUVECs seeded on 6- or 24-well plates were prepared and washed once with Opti-MEM I medium (Invitrogen). Transfection of siRNAs (100 nM) was performed with Lipofectin reagent (Invitrogen) as instructed by the manufacturer. Toxi-Blocker transfection supplement (TOYOBO) was used to prevent cytotoxicity of lipofection reagents. After 12 h of incubation, culture media were changed to endothelial growth medium-2 media, and incubation was continued for 24 h.

Luciferase Reporter Gene Assay—HEK293 cells stably transfected with human TLR2 gene (or mock control vector) were plated at 5×10^4 cells/well in 24-well plates before DNA transfection. The cells were transiently transfected with 50 ng of an NF-κB-driven firefly luciferase reporter plasmid (pNF-κB-Luc, Stratagene) and 5 ng of a construct directing expression of *Renilla* luciferase under the control of a constitutively active thymidine kinase promoter (pRL-TK, Promega). After 12 h of incubation, the cells were transfected with 100 nM siRNA oligonucleotide for MyD88 (or glyceraldehyde-3-phosphate dehydrogenase control). Toxi-Blocker transfection supplement was used to prevent cytotoxicity of lipofection reagents. After a further 24 h of incubation, the cells were stimulated with TLR2 agonists in media containing 1% fetal bovine serum for 6 h. Then the cells were lysed, and luciferase activity was measured as described previously (17, 20).

Determination of VWF, IL-8, and TNF-α by ELISA—HAECs were grown on 24-well plates, then washed and placed in 200 μl of Opti-Mem I (Invitrogen) containing 1% fetal bovine serum without growth factors, and stimulated with various concentrations of TLR2 agonists for 60 min. The amount of VWF released into the medium was measured by a VWF ELISA kit (American Diagnostica) according to the manufacturer's instructions. Results are representative of three separate experiments and expressed as means ± S.D. To clarify the mechanism by which TLR2 induces VWF exocytosis, HAECs were pretreated for 30 min with 10 μM U-73211 and then stimulated with LTA for 60 min. For other experiments, HAECs were pretreated with 10 μM BAPTA-AM for 30 min or 10 ng/ml IFN-γ for 12 h or precultured with $CaCl_2$-free DMEM for 1 h. To determine the amounts of IL-8 released, HAECs were grown on 96-well plates and then washed and placed in 200 μl of Opti-Mem I (Invitrogen) containing 1% fetal bovine serum and stimulated for 4 h with various concentrations of TLR2 agonists. The amounts of IL-8 released into the media were measured by human IL-8 Cytoset (Invitrogen) according to the manufacturer's instructions. THP-1 cells (1×10^5) were stimulated for 6 h with various concentrations of TLR2 agonists. The amounts of TNF-α released into the media were measured by human TNF-α Cytoset (Invitrogen) according to the manufacturer's instructions. Results are representative of three separate experiments and expressed as means ± S.D.

Adhesion Assay—Confluent HAECs seeded on 24-well plates were treated with 10 μg/ml LTA for 60 min. The culture medium was then removed, and monocytic THP-1 cells (2.5×10^5) prelabeled with Alexa564-conjugated concanavalin A were added to the culture. Cells were then allowed to adhere for 30 min on a rocking platform. After two washes with phosphate-buffered saline, fluorescent images were immediately obtained by a fluorescent microscope IX71 with DP70 image capture (Olympus) and processed using Adobe Photoshop, version 7.0. Adhesion of red fluorescent cells was quantified in three fields per well. Results are representative of three separate experiments and expressed as means ± S.D.

Immunofluorescence of VWF—Confluent HAECs were treated with 10 μg/ml LTA or 10 μM A23187 for 60 min. The culture media were removed, and the cells were immediately fixed at −20 °C with methanol for 60 min. Immunostaining was carried out using an anti-VWF rabbit polyclonal antibody (Santa Cruz Biotechnology, Santa Cruz, CA) and Alexa488-conjugated secondary antibody (Invitrogen). Cell nuclei were also stained with 2.5 μg/ml Höechst 33342 for 30 min. Images were obtained by a fluorescent microscope IX71 (magnification: ×40) with DP70 image capture (Olympus) in the presence of the Prolong Gold Antifade reagent (Invitrogen) and processed using Adobe Photoshop, version 7.0 (Adobe). Results are representative of three separate experiments.

Immunoblot Analysis—Confluent HAECs seeded on 60-mm plates were transfected with gene-specific siRNA and incubated in Opti-Mem I media containing 5% fetal bovine serum for 4–6 h. The cells were stimulated with 1 μg/ml LTA for 0–60 min and lysed with a buffer consisting of 20 mM Tris-hydrochloride (pH 7.2), 150 mM sodium chloride, 5 mM EDTA, and 1% Triton X-100 in the presence of protease inhibitors (Roche Applied Science) at 4 °C for 15 min followed by clarification by centrifugation at 12,000 × *g* for 10 min. SDS-PAGE and immunoblot analyses were performed as described previously (17, 20). Results are representative of three separate experiments.

Flow Cytometry—To assess the surface expression of P-selectin, confluent HAECs were treated with 10 μg/ml LTA for 30 min. To assess the surface expression of TLR2, confluent HAECs or HUVECs were treated with 10 ng/ml IFN-γ or they were incubated for 12 h under laminar flow. Cell culture under laminar flow was performed with a cone and plate apparatus as described previously (22). Magnitude of the flow was controlled at ~15 dyn/cm^2. The cells were then removed with phosphate-buffered saline containing 20 mM EDTA and fixed with phosphate-buffered saline containing 4% paraformaldehyde at 4 °C for 60 min. The cells were then incubated at 4 °C for 60 min with anti-TLR2 monoclonal antibody (IMG-319), anti-P-selectin monoclonal antibody (BD Biosciences), or isotype-matched mouse IgG and then with fluorescein isothiocyanate-conjugated anti-mouse IgG. Fluorescence was measured using a FACSCalibur (BD Biosciences).

Statistics—All values were evaluated by statistical analysis using one-way analysis of variance and Student-Newman-Keul's test. Differences were considered to be statistically significant at the level of $p < 0.05$.

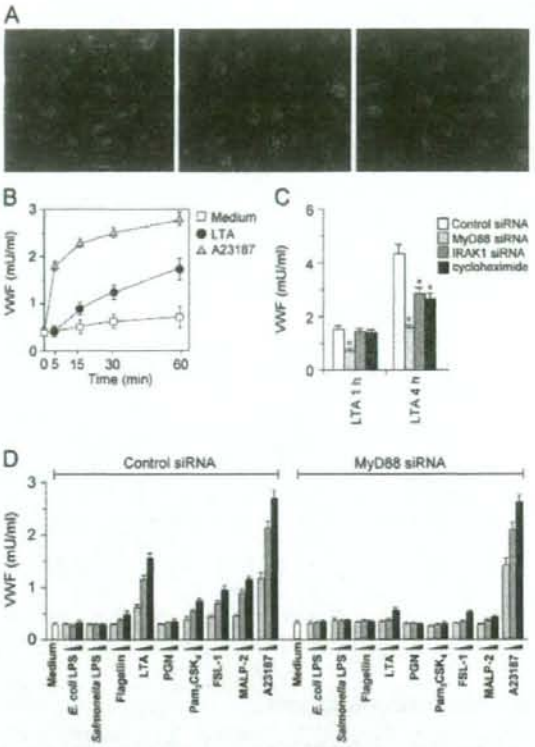

FIGURE 1. **MyD88-dependent Weibel-Palade body exocytosis by bacterial constituents.** *A*, HAECs stimulated with 10 μg/ml LTA or 1 μM A23187 for 60 min were fixed and stained immunofluorescently with anti-VWF antibody (*green*) and with Höechst33342 (*blue*). *Left*, unstimulated; *middle*, stimulated with LTA; *right*, stimulated with A23187. *B*, HAECs were stimulated with 1 μg/ml LTA or 1 μM A23187 for the indicated periods. The amounts of VWF released into the media were measured by ELISA. Each value is the mean ± S.D. ($n = 3$). *C*, HAECs transfected with MyD88 or IRAK1-specific or control siRNA were prepared. Cells were pretreated with 10 μg/ml cycloheximide for 30 min and then washed and stimulated with 10 μg/ml LTA for 60 min or 4 h. The amounts of VWF released into the media were measured by ELISA. Each value is the mean ± S.D. ($n = 3$). *, *versus* control group, $p < 0.01$. *D*, HAECs transfected with MyD88-specific or control siRNA were stimulated with *E. coli* LPS O26:B6 (0.01–1 μg/ml), LPS from *S. minnesota* (0.01–1 μg/ml), flagellin from *S. typhimurium* (0.1–10 μg/ml), LTA from *S. aureus* (0.1–10 μg/ml), PGN from *S. aureus* (0.1–10 μg/ml), Pam_3CSK_4 (0.1–10 μg/ml), FSL-1 (0.01–1 μg/ml), MALP-2 (0.01–1 μg/ml), and A23187 (0.1–10 μM) for 60 min, and then the amounts of VWF released into the media were measured. Each value is the mean ± S.D. ($n = 3$).

RESULTS

Induction of Weibel-Palade Body Exocytosis by Bacterial Constituents—We first examined whether bacterial LTA activated degranulation of Weibel-Palade bodies, because LTA has been reported to stimulate vascular endothelial cells, leading to induction of production of proinflammatory mediators, dysfunction, or cell death (23–25). After stimulation of HAECs for 30 min, LTA clearly decreased the amount of Weibel-Palade bodies, stained with an antibody to VWF, in the cells (Fig. 1*A*). Compared with the calcium ionophore (A23187)-induced response, we found that LTA gradually activated Weibel-Palade body exocytosis, quantification of which was performed by measuring the amount of VWF released into the media (Fig. 1*B*). VWF release by stimulation with